Coexistence in Periodic Environments

Alexa M Scott[1*], Carling Bieg[1,2], Bailey C McMeans[3], Kevin S McCann[1]

[1] Department of Integrative Biology, University of Guelph, Ontario, Canada

[2] Department of Ecology and Evolutionary Biology, Yale University, New Haven, Connecticut, USA

[3] Department of Biology, University of Toronto, Mississauga, Ontario, Canada

*corresponding author

ORCIDs and email addresses

*Alexa M Scott: 0000-0003-0776-0582 (ascott16@uoguelph.ca)

Carling Bieg: 0000-0003-1552-2007 (carling.bieg@gmail.com)

Bailey C McMeans: 0000-0002-9793-6811 (bailey.mcmeans@utoronto.ca)

Kevin S McCann: 0000-0001-6031-7913 (ksmccann@uoguelph.ca)

Keywords: Periodicities, species coexistence, competition, Lotka-Volterra, climate change

Word Count: 5340 (main body)

Submission Content: Main text, one table, six figures, supplementary material (4 sections)

Abstract

Climate change and other anthropogenic impacts are rapidly altering natural environmental periodicities on a variety of time scales. Despite this, a general theoretical foundation describing the role of periodic environmental variation in structuring species interactions and ecological communities is still underdeveloped. Alarmingly, this leaves us unprepared to understand and predict implications for the maintenance of biodiversity under global change. Here, we extend a two-species Lotka-Volterra competition model that incorporates periodic forcing between seasons of high and low production to investigate the effects of changing environmental patterns on species coexistence. Towards this, we define coexistence criteria for periodic environments by approximating isocline solutions akin to classical coexistence outcomes. This analytical approach illustrates that periodic environments (i.e., seasonality) in and of themselves can mediate different competitive outcomes, and these patterns are general across varying time scales. Importantly, species coexistence may be incredibly sensitive to changes in these abiotic periods, suggesting that climate change has the potential to drastically impact the maintenance of biodiversity in the future.

Introduction

Nature is abundant with a diverse array of periodic climate signals (Jackson et al. 2021; Pokorný 2021). The complex variations in temperature over time (Jiang and Morin 2007; Klausmeier 2010), for example, can be decomposed into different lengths of underlying periodicities using spectral analysis, revealing a complex mosaic of short (e.g., seconds, minutes, hours, days), medium (e.g., months, years), long (e.g., multi-decadal), and very long natural periods (e.g., 100s to 1000s of years) (Forrest and Miller-Rushing 2010; Vasconcellos et al. 2011; Huntly et al. 2021; Joseph and Kumar 2021; Pokorný 2021). The regularity of these environmental periods allows for species to adapt and respond to them (Bernhardt et al. 2020; Fretwell 1972; Shuter et al. 2012; Tonkin et al. 2017), meaning that nature has evolved around, and within, these complex temporal abiotic signatures (Mathias and Chesson 2013; Varpe 2017; Rudolf 2019). Despite the long-known recognition of nature's complex abiotic palette (White and Hastings 2020), relatively little ecological research has considered the scope of nature's abiotic variability in maintaining species diversity (Abrams 2022).

Researchers have clearly argued that temporal variation (e.g., stochasticity) can promote species coexistence via fluctuation-dependent coexistence mechanisms (e.g., storage effect, relative nonlinearity) (Chesson 2000, 2018; Adler et al. 2006; Meyer et al. 2022). With these mechanisms, temporal niche differentiation enables coexistence between species with different competitive advantages (Angert et al. 2009; Mathias and Chesson 2013; Miller and Klausmeier 2017). Despite the broad focus on environmental variation, one specific class of variability that has been less-well explored, yet ought to provide a generalizable and analytically tractable

entryway into coexistence theory for variable environments, is that of periodic fluctuations – that is, repeated and predictable fluctuations in environmental conditions. For examples, (Litchman and Klausmeier 2001) use fast/slow approximations to elegantly show that night/day oscillations in light can mediate competitive outcomes in phytoplankton – analytical solation that are tricky to garner from environmentally stochastic models.

Studies are beginning to suggest that periodic environments may have significant implications for species coexistence (Mathias and Chesson 2013; Miller and Klausmeier 2017; White and Hastings 2020). For example, temporally changing resource conditions, which fluctuate between seasons of high productivity to seasons of very little to no productivity (Fretwell 1972; Chesson and Huntly 1997), may favour different species at different times of a period (Armstrong and McGehee 1980; Litchman and Klausmeier 2001; Hastings 2012; Huntly et al. 2021). Similarly, it has been suggested that certain life history trade-offs and temporal differentiation in competing species' performance may alter coexistence outcomes in the face of periodic environments (Litchman and Klausmeier 2001; McMeans et al. 2020). Recently, Mougi (2020) extended competition results from single periodicities to polyrhythms (i.e., multiple interacting periodicities) to show that the coupling of differently timed resource fluctuations may broaden the range of coexistence between diverse species that rely on limited resources. While these recent papers highlight the importance of periodic variation, the demand for a more general theoretical understanding on the role of periodic conditions – either in isolation or as suites of periodicities (i.e., polyrhythms) – remains (White and Hastings 2020; Abrams 2022). Notably,

we lack a general understanding of coexistence in periodic environments akin to our well-established theoretical foundation framed around steady-state dynamics.

The development of such general theory is critical as climate change is currently altering the nature of these environmental fluctuations (Dijkstra et al 2011; Shuter et al. 2012; Urban et al. 2012; Chesson 2018; Al-Habahbeh et al. 2020). Northern-hemisphere winters are becoming shorter in length and more moderate (Caldwell et al. 2020; Edlund et al. 2017; Ficker et al. 2017; Warne et al. 2020), and weather patterns across the globe are becoming more variable and unpredictable (Fang and Stefan 1998; O'Reilly et al. 2015). In response, many communities have experienced an increase in species extinction (Urban et al. 2012; Moor 2017; Fung et al. 2020) and invasion rates (Stachowicz et al. 2002; Sharma et al. 2009; Dijkstra et al. 2011; Cerasoli et al. 2019; Atkinson et al. 2020). Therefore, as climate change continues to alter the abiotic conditions to which organisms have adapted to, the mechanisms regulating species coexistence may be fundamentally altered (di Paola et al. 2012; Korpela et al. 2013; Tunney et al. 2014; Anderson et al. 2015; Eloranta et al. 2016; Bartley et al. 2019; Caldwell et al. 2020). With all this in mind, developing an understanding for the mechanisms behind the maintenance of biodiversity in periodic environments becomes even more crucial.

Inspired by the fluctuating-light-driven coexistence results of Litchman and Klausmeier (2001), we sought to develop a generalizable framework for coexistence in fluctuating environments. Towards this, we extend upon the seasonal coexistence model first introduced by McMeans et al. (2020) to more broadly explore the role of periodic forcing across time scales (e.g., days to

multi-decadal) via different biological parameter combinations. We also generalized our approach by allowing high and low growth periods (not just high growth - no growth alone), with temporally-differential competitive abilities. Specifically, we extend the classical Lotka-Volterra coexistence criteria to include the role of environmental periodicities. This approach allows our results to be phrased around classical coexistence conditions with temporally-scaled inter- and intraspecific competition strengths. Here, we define a period as a unit of time that is composed of two distinct seasons of variable length and seek to generally explore which competitive outcomes may occur in these environments and under what biological conditions (i.e., different growth rates). Towards this, we employ an analytical approach consistent with the classical Lotka-Volterra phaseplane theory by developing a simple approximation that allows us to solve for the isocline solutions of a time-separated periodic model. Specifically, this approximation allows us to define coexistence criteria for periodic environments. We then illustrate how periodic environments can, in and of themselves, drive bifurcations (i.e., changing invasion criteria) such that competitive outcomes (i.e., stable coexistence, competitive exclusion, and contingent coexistence) are mediated by the environment. We end by discussing our competition results in light of how climate change is altering the nature of key underlying abiotic periodicities.

Methods

We start by extending McMeans et al. (2020)'s annual seasonal model. Here, we define season more generally as a discrete division in time that repeats itself, or is periodic, of any given length within a period. As such, summer (more productive) and winter (less productive) seasons in

McMeans et al. (2020) repeat themselves with a periodicity of one-year, but we may also similarly decompose other naturally shorter (e.g., seconds (Huntly et al. 2021)) and longer (e.g., El-Nino Southern Oscillations (Joseph and Kumar 2021)) periods of time into discrete seasons of more or less productive conditions. Towards this general understanding of periodic environments, we extend the Lotka-Volterra competition model (Chesson 2018) into a periodic model that repeatedly alternates between two discrete seasons, a productive (f_P) and less productive (f_{LP}) season. For each species, these functions are modelled with environmentally specific parameter combinations to incorporate biological constraints within each season, discussed below (Fig. 1a). The Lotka-Volterra model is defined as:

$$f_{S,j}(t) = \frac{dX_j}{dt} = r_{S,j}X_j(1 - \alpha_{S,jj}X_j - \alpha_{S,jk}X_k) \quad (1)$$

where j and k represent two competing species, and S represents a season (either productive, P, or less productive, LP). Here, $r_{S,j}$ is the intrinsic rate of population growth for species j in a season, S, $\alpha_{S,jj}$ is the intraspecific competitive coefficient for species j in season S, and $\alpha_{S,jk}$ is the interspecific competitive coefficient describing the effect of species k on species j in season S.

When running simulations, and to maintain the spirit of the model assumptions (i.e., productive and less productive season), we assumed the following simple biologically realistic assumptions:

(1) Maximal growth rates are larger in the productive season than the less productive season for both species (i.e., $r_{P,j} > r_{LP,j}$), and;

(2) Since resources are more available in the productive season compared to the less productive season, intraspecific competition will be lower in the productive season compared to the less productive season (i.e., $\alpha_{P,jj} < \alpha_{LP,jj}$).

Further, to incorporate realistic biological trade-offs between competing species, we assumed that species 1 is a better performer (in terms of growth and competition) in the productive season compared to species 2, and the opposite is true in the less productive season. Keeping in mind the previous seasonal constraints, this produces the following realistic parametric trade-offs for the two species:

(1) Species 1 has a higher growth rate in the productive season (i.e., $r_{P,1} > r_{P,2}$) and a lower growth rate in the less productive season (i.e., $r_{LP,2} > r_{LP,1}$) compared to species 2, and;

(2) Species 1 has a smaller intraspecific competitive coefficient in the productive season (i.e., $\alpha_{P,11} < \alpha_{P,22}$) and a larger intraspecific competitive coefficient in the less productive season (i.e., $\alpha_{LP,11} > \alpha_{LP,22}$) compared to species 2.

These trade-offs are similar to an empirical case study by McMeans et al. (2020) where cold-adapted fish (e.g., lake trout, *Salvelinus namaycush*) are seasonal generalists with moderate growth rates year-round, and warm-adapted fish (e.g., smallmouth bass, *Micropterus dolomieu*), the lake trout's competitor, are seasonal specialists with higher growth rates during the summer and lower growth rates during the winter. Note that we have not set any seasonal constraints on the interspecific competitive coefficients, therefore, $\alpha_{S,jk}$ can be any value.

With the above assumptions taken into consideration, our model is a periodic step function (repeats every 1-time unit, or period) that goes through a productive season (*P*), and a less productive season (*LP*), as follows:

$$\frac{dX_j}{dt} = \begin{cases} f_{P,j}(t) & i < t < i + \tau p \\ f_{LP,j}(t) & i + \tau p < t < i + \tau \end{cases} \quad (2)$$

Where i is the period number (i.e. year) that runs on an integer step size of 1 from 0 to t_{prd} (the number of periods that the model runs for). τ governs the length of each period, and p is the proportion of each period that is considered productive (i.e., τp is the length of the productive season; leaving $\tau(1\text{-}p)$ as the length of the less productive season). The period length, defined by τ, allows us to examine how environmental periodicities, and associated biological trade-offs, across time scales may influence coexistence. As above, j represents one of the two competitive species, either species 1 or 2. These periodic functions of f_P and f_{LP} are defined in equation (1) as f_S.

We coded all numerical simulations in Mathematica 12.0. The models are integrated over numerous periods until an asymptotic state, referred to hereafter as an equilibrium state, despite within-period variation, has been reached (i.e., mean value from 900 – 1000 time-units) to remove transient influences. However, within each time unit, as discussed above, they sequentially follow first productive then less productive parameters corresponding to the given productive seasonal fraction, p, within the period. The productive seasonal fraction, p, allows us to change the proportion of the period that is under our productive conditions versus our less productive conditions, $(1\text{-}p)$ (e.g., increase f_P) (Fig. 1b).

Finally, all model parameterizations for our simulations can be found in our figure legends and in the Supplementary Material. Below we first walk through our approximation and then our general analytical results before highlighting the generality of our analytical solutions using numerical simulations. For each outcome, we explore how changing the season lengths, via p, influences competitive coexistence and exclusion (Fig. 1b; Table 1).

Results

Here, we present our approximated isocline solutions and investigate the resulting coexistence criteria and behaviour under seasonality. Next, we reveal that changing season length, p, in response to climate change, mediates coexistence, competitive exclusion, and contingent coexistence (Fig. 3). Finally, we explore the robustness of our seasonally-mediated outcomes (i.e., seasonally-driven bifurcations) across a range of period lengths (Figs. 4-6).

Approximate Isocline Solutions for the Periodic Lotka-Volterra Model

Although we use a periodically forced system, we can use equilibrium concepts to understand the dynamics of our model. Specifically, our model reaches an attractor such that the densities fluctuate modestly up and down on the attractor around a mean that does not change (i.e., an asymptotic state or dynamic equilibrium; Fig.S2.2). Given this equilibrium-like dynamic, we are interested in considering this asymptotic behaviour in a manner similar to the way we would for a system that reaches a true equilibrium. Here, we provide an approximation for our model isoclines and equilibria that mirror those of the original Lotka-Volterra competition model.

Note that the isoclines can be solved by recognizing that each period of τ time units would necessarily have to result in zero net growth (i.e., no overall changes in density between the start and end of each period), akin to classical zero-growth isoclines with a deterministic equilibrium. That is, from System (2), the X_j zero-net-growth condition occurs when $\frac{dx_j}{dt} = 0$. From this, the isocline solution follows as:

$$\int_0^{\tau p} f_{P,j}(t) = -\int_{\tau p}^{\tau} f_{LP,j}(t) \tag{3}$$

This isocline solution (3) is not analytically tractable (note that each season has dynamics over a time interval), making it seem as though an isocline approach appears infeasible.

Towards solving for an approximation for periodically forced isoclines, we take a slightly different approach then the classical linearization of the full equations (see Litchman and Klausmeier (2001) for an example). As our model is not tractable with this approach, we instead proceed by assuming that we can find a linearized approximation to the isocline from the periodic model by searching for points in phase space where the linearization of each seasons' dynamics are exactly negated by each other (for both the X_1 and X_2 isoclines). We define such points as **zero net growth** points in the phaseplane (i.e., a point on the forced model's isocline) and we define the collection of these points as **the linearized isocline approximation of the periodically-forced model**. Clearly, as the length of the period, τ, goes to 0, the error in this linear approximation will also go to 0. However, for longer periods or large growth rates (r), non-linear dynamics may drive this simplification to work poorly (see Supplementary Material

S4). Because of this, we numerically check our analytical results with numerical calculations throughout. We note that despite this, the results work surprisingly well across large parameter values suggesting the linear approximation works even when some degree of nonlinear dynamics are expressed.

By assuming that the instantaneous rates of change for each species at this X_1-X_2 co-ordinate are linear, we approximate the dynamics over the time period, τ, by solving the equations using the Fundamental Theorem of Calculus over each period (see Supplementary Material S1). That is, over the interval fraction, τp, the productive trajectory scales linearly on the co-ordinate X_1-X_2 as:

$$\frac{dX_1}{dt} = \tau p f_{P,1}(X_1, X_2) \tag{4}$$

and the less productive trajectory over the interval fraction $\tau(1\text{-}p)$ scales linearly as:

$$\frac{dX_1}{dt} = \tau(1-p) f_{LP,1}(X_1, X_2) \tag{5}$$

Given Equations (4) and (5), then the linearized dynamics at a X_1-X_2 co-ordinate negate each other (i.e., resulting in the X_1-isocline) when:

$$\tau p f_{P,1}(X_1, X_2) = -\tau(1-p) f_{LP,1}(X_1, X_2) \tag{6}$$

This approximation (Equation (6)), if it works, can be solved symbolically as done elegantly for the classical Lotka-Volterra model and thus allows an entry point into well-known coexistence analyses and interpretations.

From Equation (6), we see that τ factors out. After substituting the productive and less productive models of Equation (1) into Equation (6) and then some algebra, the resulting isocline solutions, for both species, follow the following form:

$$X_1 = -\frac{pr_{P,1}\alpha_{P,12} + (1-p)r_{LP,1}\alpha_{LP,12}}{pr_{P,1}\alpha_{P,11} + (1-p)r_{LP,1}\alpha_{LP,11}} X_2 + \frac{pr_{P,1} + (1-p)r_{LP,1}}{pr_{P,1}\alpha_{P,11} + (1-p)r_{LP,1}\alpha_{LP,11}} \quad (7)$$

The geometry of the approximated isoclines (Equation (7)) resembles that of the original Lotka-Volterra isoclines, which therefore allows us to identify general rules for coexistence in periodic environments akin to the original coexistence criteria (Fig. 2a). Here, the isocline approximation solutions (and therefore coexistence criteria) are now based on temporal-growth-scaled inter- versus intra-specific competition rates (whereas the original Lotka-Volterra conditions are not dependent on growth rates; see Table 1 for Lotka-Volterra vs. Seasonal Coexistence Criteria). Thus, the approximation enables us to generally determine and graphically explore how periodic environments and biological rates may interact in regulating competitive outcomes (Fig. 2b). Immediately, based on these conditions, we can see that the duration of each season, and the corresponding biological conditions within them, play a critical role in regulating competitive outcomes in periodic environments. That is, our parameter *p* may drive bifurcations, and therefore alter competitive outcomes under changing climatic conditions (Fig. 2b).

We found numerically that this approximation works quite well (see Supplementary Material S2 for examples) and was, for example, able to repeatedly and accurately calculate the transcritical bifurcation points where an interior equilibrium intersects and exchanges stability, with an axial solution. Other approaches similar to our approximation, such as Litchman and Klausmeier

241 (2001), have been used to accurately investigate species coexistence when organismal dynamics
242 are fast relative to their forcing speed. Given our assumption of linearity, the relative time scale
243 of forcing vs. dynamics ought to be important for our approximation's accuracy. Indeed, when
244 either the period length (τ) or the growth rate (r) becomes larger, the apparent length of each
245 period increases, allowing for more nonlinearity within each season's dynamics, which results in
246 the approximation to fail at predicting the asymptotic behaviour (see Supplementary Material
247 S4). Nevertheless, the range at which this approximation holds is impressively robust.
248
249 **General outcomes of changing environments**
250 Given that changing season lengths may have powerful implications for species coexistence, we
251 now ask how changing season length, p, (i.e., altering seasonal asymmetry) affects competitive
252 outcomes. To do this we vary the season length from p=0 (i.e., the full period being entirely less
253 productive) to p=1 (i.e., the full period being entirely productive). We note that these endpoints
254 (i.e., p=0 or p=1) are constant (i.e., no seasonality) and thus, they reduce to the classic Lotka-
255 Volterra coexistence criteria based on the individual biological conditions for P or LP (Table 1).
256 These endpoints also give us reference conditions for exploring the effects of environmental
257 periodicity and seasonally-mediated coexistence outcomes.
258
259 Since McMeans et al. (2020) found the intriguing case of seasonally-mediated coexistence, we
260 were interested in using our analytical results to unpack other examples of how seasonal change
261 could fundamentally alter competitive outcomes. McMeans et al. (2020) noted that where the
262 boundary conditions yielded competitive exclusion (i.e., exclusion at p=0 and p=1), a seasonal

263 model could produce coexistence for intermediate *p*-values. This is intriguing as it immediately
264 suggests that alterations in *p* (say from climate change) can drive exclusion. Importantly, our
265 analytical solutions (Table 1) suggest that seasonality can mediate all possible competitive
266 outcomes at intermediate *p*-values (Fig. 3). Indeed, we found seasonally-mediated coexistence,
267 competitive exclusion, and contingent coexistence (i.e., alternative states) (Fig. 3a-c
268 respectively).
269
270 For these seasonally-mediated outcomes, when the qualitative competitive outcome at
271 intermediate *p* is fundamentally different from the extremes (i.e., $p = 0$ and 1), *p* drives a series
272 of transcritical bifurcations that move the system between different conditions in Table 1 (shifts
273 between shaded and clear zones indicate transcritical bifurcations that alter the qualitative nature
274 of the attractor in Fig. 3). Specifically, under our given sets of parametric combinations,
275 changing *p* always drives a series of two bifurcations for these seasonally-mediated outcomes
276 (Fig. 3). Other competitive outcomes of course are seasonally sensitive as they result in *p*-driven
277 bifurcations when coexistence outcomes transition between the two endpoint conditions.
278 Additionally, we note that these transcritical bifurcations can be considered as changes in the
279 invasion criteria – in this case, seasonally-altered invasion criterion – as they are commonly
280 referred to in competition theory. For example, in Fig. 3a, the gray shaded regions indicate that
281 one species cannot invade from small densities while in the white or unshaded region, it
282 suddenly can invade from small densities.
283

Finally, clearly not all parameter combinations are sensitive to *p*-driven bifurcations. In these cases, *p* may simply drive changes in species' densities rather than shifts in the equilibrium structure (e.g., as seen in McMeans et al. (2020)). While here we broadly unpack *p*-driven bifurcations to explore the generality of these outcomes, we note that all results below have nearby solutions that do not undergo bifurcations yet and are qualitatively similar in terms of the general effect of *p* on the isocline and equilibrium geometry.

Robustness of Seasonally-Mediated Competitive Outcomes

To fully understand how robust the different seasonally-mediated outcomes are we looked at the bifurcation structure in 2-dimensional parameter space, by using both season length, *p*, (as in Fig. 3) and the period length, τ, as bifurcation parameters. We note that if seasonally-mediated outcomes exist across a broad range of period lengths, τ, then this suggests that seasonally-mediated competitive outcomes could be found across a wide range of natural periodicities (from diurnal to multi-decadal).

In Fig. 4a, we document cases where a lack of periodicity (i.e., at p=0 or 1) drives competitive exclusion while for a broad range of τ's (ranging from 1-100 time units), we have species coexistence at intermediate *p*-values. Our analytical solutions allow us to track the "mean equilibrium" through each transcritical bifurcation from competitive exclusion of species 1 to species coexistence and finally to competitive exclusion of species 2 as the length of the productive period, *p*, increases (i.e., changing *p* shifts between competitive exclusion and stable coexistence conditions in Table 1; Figs. 4bi-iii, S3.1). The robustness of this pattern implies that

for any given τ, seasonality alone can mediate coexistence at intermediate p-values. As the period length (τ) grows, the numerically-generated region of coexistence broadens, and the second transcritical bifurcation point, the transition between species coexistence and competitive exclusion of species 2, deviates away from the analytically-determined transcritical bifurcation point (see more regarding approximation accuracy of seasonally mediated coexistence in S4.1). This suggests that the analytical bifurcation structure is sensitive to different parametric values (which is also suggested by the seasonal coexistence criteria shown in Table 1), but nonetheless, the result of seasonally-mediated coexistence is qualitatively general. We note that the simple linear prediction breaks down as $r\tau$ grows (i.e., larger τr allows the nonlinear dynamics to express themselves; see Supplementary Material S4.1). Thus, we see that seasonally-mediated coexistence occurs very broadly suggesting that a large range of natural periodicities may be powerful drivers of coexistence.

Similarly, in Fig. 5a, we document cases where species coexistence occurs in static environments (i.e., at p=0 or 1), while competitive exclusion occurs at intermediate p-values over a broad range of τ's (here, from 1-40 time units). Following McMeans et al. (2020)'s naming convention, we refer to this as seasonally-mediated competitive exclusion. As in the above case, with increasing p, our analytical approximation tracks the isoclines and the "mean equilibrium" from stable coexistence to competitive exclusion of species 2 through a transcritical bifurcation on the X_2=0 axis, and finally back through the axis (via another bifurcation) to stable coexistence (Figs. 5b, S3.2). The transcritical bifurcations points determined by our analytical solution accurately track the numerical solutions over several period length values of τ before the seasonal bifurcations

cease at higher values of τ. Again, we note that the simple linear prediction breaks down as τr grows (i.e., larger τr allows the nonlinear dynamics to express themselves; see Supplementary Material S4.2). The 2-dimensional bifurcation diagram again shows a broad range in τ-values that yield competitive exclusion; however, it does not stretch across all τ-values (i.e., very large period lengths). While the exact range of parameter space that this seasonally-mediated competitive exclusion occurs at is clearly dependent on other parameters, this result is still quite general over a wide range of τ-values, suggesting that periodic environments may also be powerful drivers of competitive exclusion. Here, as τ grows, this tongue of competitive exclusion slowly shrinks across intermediate values of p. Again, this is an interesting result, which suggests that simple alterations in season length may fundamentally alter competitive outcomes.

Finally, in Fig. 6a, similar to the above seasonally-mediated coexistence case with competitive exclusion at the boundaries (i.e., p=0 or 1), we now document cases where contingent coexistence (i.e., alternative states) occurs at intermediate p values across a broad range of τ's (here, from 1-100 time units). Although this outcome is quite similar to seasonally-mediated coexistence with competitive exclusion being located at each boundary (i.e., p=0 or 1), its isocline geometry, based off of parametric combinations, results in seasonally-mediated contingent coexistence at intermediate p-values (Figs. 6bi-iii, S3.3). Our approximation tracks the analytical non-trivial (interior) equilibrium, which in this case is unstable in positive (X_1, X_2) state space (Fig. 6bii). Here, initial densities determine which species will dominate and which species will become extinct with time (i.e., which of the two stable axial solutions, shown in Fig.

6bii, the system will end up at). The robustness of this pattern also implies that for any given τ, seasonality may be a powerful driver of contingent coexistence (i.e., changing p moves from competitive exclusion to contingent coexistence conditions in Table 1). As τ grows, the numerically-generated contingent coexistence region expands across higher productive season lengths before it narrows around lower lengths of the productive season. Again, our analytical solution accurately determines at which p values the transcritical bifurcations will occur for very small τ values, but falls off with larger period lengths, τ (see Supplementary Material S4.3 for approximation accuracy of seasonally mediated contingent coexistence), despite the general phenomenon remaining across time scales.

These three seasonally-mediated outcomes suggest that seasonal alterations, due to climate change, may drive precipitous changes in competitive systems. All of these seasonally-mediated outcomes appear general and may be found across various ecosystems that experience abiotic fluctuations of any period length. Similarly, for a given period length (e.g., annual variation), these outcomes may be highly general for competing organisms with a range of life history strategies (i.e., vital rates that dictate the speed of biotic dynamics relative to any environmental variation). On the other hand, depending on parametric values, not all instances of periodic variation will drive these series of bifurcations. Under some conditions, there are simply p-driven changes in species densities between the boundary conditions where only one bifurcation (Figs. S2.1e, S2.1f) or no bifurcations (Figs. S2.1d) are found under changing periodicities.

Discussion

Here, we present a linear approximation similar in approach to other periodic models (e.g., Han et al. (1999); Litchman and Klausmeier (2001)) to analytically solve for a periodic Lotka-Volterra competition model (see Table 1 for seasonal coexistence criteria). Our linear approximation quantitatively breaks down for large values in τr but still largely operates to qualitatively predict the nature of periodic-forcing on competition (e.g., Fig. 4a,6a). This approximation, akin to the longstanding classical Lotka-Volterra coexistence conditions, importantly allows us to derive a parallel set of coexistence conditions for periodic environments. With the inclusion of periodic environmental forcing, we find that species coexistence depends on seasonal-growth-scaled inter- versus intra-specific competition strengths (Table 1). That is, where classical stable coexistence requires intraspecific competition to be greater than interspecific competition, for both species, we show that intraspecific competition, scaled by seasonal growth, must be greater than interspecific competition, scaled by seasonal growth, for both species.

These seasonal coexistence conditions importantly suggest that species' coexistence may be incredibly sensitive to changes in season length. While McMeans et al. (2020) found seasonally-mediated coexistence through empirically-motivated numerical simulations, our results show that seasonality can mediate coexistence, competitive exclusion, and contingent coexistence (Fig. 3). That is, seasonality, in and of itself, can drive all possible competitive outcomes (i.e., Table 1). As these seasonally-mediated outcomes appear across a vast range of period lengths (Fig. 4-6), this suggests that these seasonally-mediated outcomes are quite robust, and can be found across a

392 wide range of different temporal scales and life history strategies (i.e., fast vs. slow life history
393 strategies).
394
395 As the change in season length (p) may have an important role in mediating competitive
396 outcomes (Fig. 3), climate change is altering environmental periodicities across a range of
397 temporal scales (Dijkstra et al. 2011; Shuter et al. 2012; Urban et al. 2012; Chesson 2018; Al-
398 Habahbeh et al. 2020), and our results suggest that this could have sudden and drastic –
399 sometimes unpredictable – effects on coexistence. Often the responses to changing seasons are
400 nonlinear, and some of these outcomes are unexpected based on the classical Lotka-Volterra
401 conditions under non-seasonal environments (e.g., nonlinear paths between the boundary
402 conditions at $p = 0$ and 1; Figs. 3b, 5, S2.1b and d). As an example, we find cases where
403 competitive exclusion occurs under intermediate season lengths, even though coexistence is
404 expected under the same non-seasonal conditions (i.e., coexistence occurs for entirely low- or
405 entirely high-productive conditions; Fig. 3b). Alarmingly, these strong nonlinear effects of
406 changing season length, p, suggest that precipitous changes in species density and composition
407 may unexpectedly occur as climate change alters the nature of seasonality.
408
409 Although simple, the seasonal competition model we examined here is based on biologically
410 realistic assumptions about competitive species in temporally varying environments. First,
411 periodic environments are commonly reflected by times of high and low productivity, where
412 species tend to flourish during the productive seasons, and decline (e.g., mortality-dominated)
413 during the less productive seasons as resource availability becomes sparse (Fretwell 1972;

Litchman and Klausmeier 2001; Mutze 2009; Klausmeier 2010; Hastings 2012; Lyu et al. 2016; Vihtakari et al. 2016). These periods therefore impact species' growth rates, but also offer the potential for differential responses of competing species to seasonally-driven environmental variation (Chesson and Huntly 1997; Forrest and Miller-Rushing 2010; Shuter et al. 2012; Gao et al. 2016; Chesson 2018; Huang et al. 2019). It is well known that competing species can display temporal trade-offs in stochastic environments that can promote coexistence (Angert et al. 2009; Shuter et al. 2012; Mougi 2020). For instance, Litchman and Klausmeier (2001) discovered that slow fluctuations in light promote stable coexistence between competing species of phytoplankton who exhibit trade-offs in performance across temporally changing resource availability. More recently, and consistent with our theoretical results here, empirical evidence is beginning to suggest species may show trade-offs to regular seasonal fluctuations that might promote coexistence. For example, a species may be a seasonal specialist (e.g., display a very high growth rate during the summer and a low growth rate during the winter) while its competitor may be more of a temporal generalist, who's able to maintain roughly the same growth rate year-round (Niiyama 1990; Chan et al. 2009; Abrams et al. 2013; Korpela et al. 2013; Meyer et al. 2022).

While we concentrate on temporal forcing in our model, seasonal signals in competition may often be related to spatial-temporal and behavioural patterns that govern species' competitive outcomes (McMeans et al. 2020). As an example, in some cases, species may migrate (Holt and Fryxell 2011; Teitelbaum et al. 2015; Tavecchia et al. 2016; le Corre et al. 2020; Moorter et al. 2021) or hibernate (Campbell et al. 2008; Giraldo-Perez et al. 2016) during less productive

436 seasons, opting out of competition when resources are scarce (Suski and Ridgway 2009). These
437 behavioural strategies may counteract potential negative effects of periodic variation to some
438 extent and thus promote coexistence by reducing competitive interactions during unfavourable
439 times. More empirical research is needed to further understand these spatial and behavioural
440 strategies, and seasonal trade-offs between competitive species, in order to understand their
441 mechanistic role in maintaining biodiversity with climate change.
442
443 As nature abounds with temporal variation, grasping a better understanding of coexistence
444 mechanisms in these fluctuating environments is now even more crucial with climate change.
445 We have provided an analytical solution to begin understanding these effects. Our research has
446 uncovered three competitive outcomes that could be found across a large range of natural
447 periodicities and life history strategies. As species coexistence appears to be incredibly sensitive
448 to periodic variation, climate change has the potential to drastically impact future competitive
449 outcomes in the natural world.
450
451 **Acknowledgements**

452 We would like to thank Cortland K. Griswold for his comments and suggestions that helped
453 improve this manuscript. We would also like to thank the University of Guelph's Elgin Card
454 Scholarship in Terrestrial Ecology (Grant number [I5023]) awarded to AMS, and the NSERC
455 Discovery Grant granted to KSM (Grant number [400353]) for funding this research.

Code accessibility

All code to reproduce the above analyses and figures have been archived on Zenodo (version 1.0).

459 **Literature Cited**

460 Abrams PA (2022) Competition in seasonal environments. In: Competition Theory in Ecology.
461 Oxford University Press, pp 171–208

462 Abrams PA, Tucker CM, Gilbert B (2013) Evolution of the storage effect. Evolution (N Y)
463 67:315–327. https://doi.org/10.1111/j.1558-5646.2012.01756.x

464 Adler PB, HilleRisLambers J, Kyriakidis PC, et al (2006) Climate variability has a stabilizing
465 effect on the coexistence of prairie grasses. Proc Natl Acad Sci U S A 103:12793–12798.
466 https://doi.org/10.1073/pnas.0600599103

467 Al-Habahbeh AK, Kortsch S, Bluhm BA, et al (2020) Arctic coastal benthos long-term responses
468 to perturbations under climate warming. Philos Trans A Math Phys Eng Sci 378:20190355.
469 https://doi.org/10.1098/rsta.2019.0355

470 Anderson KD, Heron SF, Pratchett MS (2015) Species-specific declines in the linear extension
471 of branching corals at a subtropical reef, Lord Howe Island. Coral Reefs 34:479–490.
472 https://doi.org/10.1007/s00338-014-1251-1

473 Angert AL, Huxman TE, Chesson P, Venable DL (2009) Functional tradeoffs determine species
474 coexistence via the storage effect. Proc Natl Acad Sci U S A 106:11641–11645.
475 https://doi.org/10.1073/pnas.0904512106

476 Armstrong RA, McGehee R (1980) Competitive Exclusion. American Society of Naturalist
477 115:151–170

478 Atkinson J, King NG, Wilmes SB, Moore PJ (2020) Summer and winter marine heatwaves favor
479 an invasive over native seaweeds. J Phycol 56:1591–1600.
480 https://doi.org/10.1111/jpy.13051

481 Bartley TJ, McCann KS, Bieg C, et al (2019) Food web rewiring in a changing world. Nat Ecol
482 Evol 3:345–354. https://doi.org/10.1038/s41559-018-0772-3

483 Bernhardt J, O'Connor M, Sunday J, Gonzalez A (2020) Life in fluctuating environments. Philos
484 Trans R Soc Lond B Biol Sci 375:1–22. https://doi.org/10.32942/osf.io/dgmr4

485 Caldwell TJ, Chandra S, Feher K, et al (2020) Ecosystem response to earlier ice break-up date:
486 Climate-driven changes to water temperature, lake-habitat-specific production, and trout
487 habitat and resource use. Glob Chang Biol 26:5475–5491.
488 https://doi.org/10.1111/gcb.15258

489 Campbell HA, Fraser KPP, Bishop CM, et al (2008) Hibernation in an Antarctic fish: On ice for
490 winter. PLoS One 3:. https://doi.org/10.1371/journal.pone.0001743

Cerasoli F, Iannella M, Biondi M (2019) Between the hammer and the anvil: How the combined effect of global warming and the non-native common slider could threaten the european pond turtle. Management of Biological Invasions 10:428–448. https://doi.org/10.3391/mbi.2019.10.3.02

Chan B, Durrett R, Lanchier N (2009) Coexistence for a multitype contact process with seasons. Annals of Applied Probability 19:1921–1943. https://doi.org/10.1214/09-AAP599

Chesson P (2018) Updates on mechanisms of maintenance of species diversity. Journal of Ecology 106:1773–1794. https://doi.org/10.1111/1365-2745.13035

Chesson P (2000) Mechanisms of maintenance of speacies diversity. Annu Rev Ecol Syst 31:343–366. https://doi.org/10.1146/annurev.ecolsys.31.1.343

Chesson P, Huntly N (1997) The roles of harsh and fluctuating conditions in the dynamics of ecological communities. Am Nat 150:519–553

di Paola A, Valentini R, Paparella F (2012) Climate change threatens coexistence within communities of mediterranean forested wetlands. PLoS One 7:. https://doi.org/10.1371/journal.pone.0044727

Dijkstra JA, Westerman EL, Harris LG (2011) The effects of climate change on species composition, succession and phenology: A case study. Glob Chang Biol 17:2360–2369. https://doi.org/10.1111/j.1365-2486.2010.02371.x

Edlund MB, Almendinger JE, Fang X, et al (2017) Effects of climate change on lake thermal structure and biotic response in northern wilderness lakes. Water (Basel) 9:1–35. https://doi.org/10.3390/w9090678

Eloranta AP, Helland IP, Sandlund OT, et al (2016) Community structure influences species' abundance along environmental gradients. Journal of Animal Ecology 85:273–282. https://doi.org/10.1111/1365-2656.12461

Fang X, Stefan HG (1998) Potential climate warming effects on ice covers of small lakes in the contiguous U.S. Cold Reg Sci Technol 27:119–140. https://doi.org/10.1016/S0165-232X(97)00027-X

Ficker H, Luger M, Gassner H (2017) From dimictic to monomictic: Empirical evidence of thermal regime transitions in three deep alpine lakes in Austria induced by climate change. Freshw Biol 62:1335–1345. https://doi.org/10.1111/fwb.12946

Forrest J, Miller-Rushing AJ (2010) Toward a synthetic understanding of the role of phenology in ecology and evolution. Philosophical Transactions of the Royal Society B: Biological Sciences 365:3101–3112. https://doi.org/10.1098/rstb.2010.0145

Fretwell SD (1972) Populations in a seasonal environment. Princeton University Press

525 Fung T, Chisholm RA, Anderson-Teixeira K, et al (2020) Temporal population variability in
526 local forest communities has mixed effects on tree species richness across a latitudinal
527 gradient. Ecol Lett 23:160–171. https://doi.org/10.1111/ele.13412

528 Gao G, Ponsard S, Lu Z, et al (2016) Different thermal responses in two coexisting aphids may
529 account for differences in their seasonal abundance in cotton fields. Int J Pest Manag
530 62:288–294. https://doi.org/10.1080/09670874.2016.1185551

531 Giraldo-Perez P, Herrera P, Campbell A, et al (2016) Winter is coming: Hibernation reverses the
532 outcome of sperm competition in a fly. J Evol Biol 29:371–379.
533 https://doi.org/10.1111/jeb.12792

534 Han BP, Virtanen M, Koponen J, Straškraba M (1999) Predictors of light-limited growth and
535 competition of phytoplankton in a well-mixed water column. J Theor Biol 197:439–450.
536 https://doi.org/10.1006/jtbi.1998.0885

537 Hastings A (2012) Temporally varying resources amplify the importance of resource input in
538 ecological populations. Biol Lett 8:1067–1069. https://doi.org/10.1098/rsbl.2012.0669

539 Holt RD, Fryxell JM (2011) Theoretical reflections on the evolution of migration. In: Milner-
540 Gulland EJ, Fryxell JM, Sinclaire ARE (eds) Animal migration. Oxford University Press,
541 New York, pp 17–31

542 Huang L, Xue W, Herben T (2019) Temporal niche differentiation among species changes with
543 habitat productivity and light conditions. Journal of Vegetation Science 30:438–447.
544 https://doi.org/10.1111/jvs.12741

545 Huntly N, Freischel AR, Miller AK, et al (2021) Coexistence of "cream skimmer" and "crumb
546 picker" phenotypes in nature and in cancer. 9:1–18.
547 https://doi.org/10.3389/fevo.2021.697618

548 Jackson MC, Pawar S, Woodward G (2021) The temporal dynamics of multiple stressor effects:
549 From individuals to ecosystems. Trends Ecol Evol 36:402–410.
550 https://doi.org/10.1016/j.tree.2021.01.005

551 Jiang L, Morin PJ (2007) Temperature fluctuation facilitates coexistence of competing species in
552 experimental microbial communities. Journal of Animal Ecology 76:660–668.
553 https://doi.org/10.1111/j.1365-2656.2007.01252.x

554 Joseph D, Kumar VS (2021) Response of ocean surface waves to the co-occurrence of Boreal
555 Summer Intra-Seasonal Oscillation and El Niño Southern Oscillation. Clim Dyn 57:1155–
556 1171. https://doi.org/10.1007/s00382-021-05763-3

557 Klausmeier CA (2010) Successional state dynamics: A novel approach to modeling
558 nonequilibrium foodweb dynamics. J Theor Biol 262:584–595.
559 https://doi.org/10.1016/j.jtbi.2009.10.018

Korpela K, Delgado M, Henttonen H, et al (2013) Nonlinear effects of climate on boreal rodent dynamics: Mild winters do not negate high-amplitude cycles. Glob Chang Biol 19:697–710. https://doi.org/10.1111/gcb.12099

le Corre M, Dussault C, Côté SD (2020) Where to spend the winter? The role of intraspecific competition and climate in determining the selection of wintering areas by migratory caribou. Oikos 129:512–525. https://doi.org/10.1111/oik.06668

Litchman E, Klausmeier CA (2001) Competition of phytoplankton under fluctuating light. American Naturalist 157:170–187. https://doi.org/10.1086/318628

Lyu L, Deng X, Zhang Q bin (2016) Elevation pattern in growth coherency on the southeastern Tibetan Plateau. PLoS One 11:1–15. https://doi.org/10.1371/journal.pone.0163201

Mathias A, Chesson P (2013) Coexistence and evolutionary dynamics mediated by seasonal environmental variation in annual plant communities. Theor Popul Biol 84:56–71. https://doi.org/10.1016/j.tpb.2012.11.009

McMeans BC, McCann KS, Guzzo MM, et al (2020) Winter in water: Differential responses and the maintenance of biodiversity. Ecol Lett 23:922–938. https://doi.org/10.1111/ele.13504

Meyer I, Steinmetz B, Shnerb NM (2022) How the storage effect and the number of temporal niches affect biodiversity in stochastic and seasonal environments. PLoS Comput Biol 18:1–21. https://doi.org/10.1371/journal.pcbi.1009971

Miller ET, Klausmeier CA (2017) Evolutionary stability of coexistence due to the storage effect in a two-season model. Theor Ecol 10:91–103. https://doi.org/10.1007/s12080-016-0314-z

Moor H (2017) Life history trade-off moderates model predictions of diversity loss from climate change. PLoS One 12:1–21. https://doi.org/10.1371/journal.pone.0177778

Moorter B van, Singh NJ, Rolandsen CM, et al (2021) Seasonal release from competition explains partial migration in European moose. Oikos 130:1548–1561. https://doi.org/10.1111/oik.07875

Mougi A (2020) Polyrhythmic foraging and competitive coexistence. Sci Rep 10:1–7. https://doi.org/10.1038/s41598-020-77483-3

Mutze GJ (2009) Changes in body condition and body size affect breeding and recruitment in fluctuating house mouse populations in south-eastern Australia. Austral Ecol 34:278–293. https://doi.org/10.1111/j.1442-9993.2008.01929.x

Niiyama K (1990) The role of seed dispersal and seedling traits in colonization and coexistence of Salix species in a seasonally flooded habitat. Ecol Res 5:317–331

O'Reilly CM, Sharma S, Gray DK, et al (2015) Rapid and highly variable warming of lake surface waters around the globe. Geophys Res Lett 42:10773–10781. https://doi.org/10.1002/2015GL066235

Pokorný V (2021) Polyrhythmic arrangements: Rhythm as a dynamic principle in the constitution of environments. Open Philosophy 4:394–403. https://doi.org/10.1515/opphil-2020-0192

Rudolf VHW (2019) The role of seasonal timing and phenological shifts for species coexistence. Ecol Lett 22:1324–1338. https://doi.org/10.1111/ele.13277

Scranton K, Vasseur DA (2016) Coexistence and emergent neutrality generate synchrony among competitors in fluctuating environments. Theor Ecol 9:353–363. https://doi.org/10.1007/s12080-016-0294-z

Sharma S, Jackson DA, Minns CK (2009) Quantifying the potential effects of climate change and the invasion of smallmouth bass on native lake trout populations across Canadian lakes. Ecography 32:517–525. https://doi.org/10.1111/j.1600-0587.2008.05544.x

Shuter BJ, Finstad AG, Helland IP, et al (2012) The role of winter phenology in shaping the ecology of freshwater fish and their sensitivities to climate change. Aquat Sci 74:637–657. https://doi.org/10.1007/s00027-012-0274-3

Stachowicz JJ, Terwin JR, Whitlatch RB, Osman RW (2002) Linking climate change and biological invasions: Ocean warming facilitates nonindigenous species invasions. Proc Natl Acad Sci U S A 99:15497–15500. https://doi.org/10.1073/pnas.242437499

Suski CD, Ridgway MS (2009) Winter biology of centrarchid fishes. In: Cooke SJ, Philipp DP (eds) Centrarchid Fishes. Blackwell Publishing Ltd., pp 264–292

Tavecchia G, Tenan S, Pradel R, et al (2016) Climate-driven vital rates do not always mean climate-driven population. Glob Chang Biol 22:3960–3966. https://doi.org/10.1111/gcb.13330

Teitelbaum CS, Fagan WF, Fleming CH, et al (2015) How far to go? Determinants of migration distance in land mammals. Ecol Lett 18:545–552. https://doi.org/10.1111/ele.12435

Tonkin JD, Bogan MT, Bonada N, et al (2017) Seasonality and predictability shape temporal species diversity. Ecology 98:1201–1216. https://doi.org/10.1002/ecy.1761

Tredennick AT, Adler PB, Adler FR (2017) The relationship between species richness and ecosystem variability is shaped by the mechanism of coexistence. Ecol Lett 20:958–968. https://doi.org/10.1111/ele.12793

Tunney TD, McCann KS, Lester NP, Shuter BJ (2014) Effects of differential habitat warming on complex communities. Proc Natl Acad Sci U S A 111:8077–8082. https://doi.org/10.1073/pnas.1319618111

627 Urban MC, de Meester L, Vellend M, et al (2012) A crucial step toward realism: Responses to
628 climate change from an evolving metacommunity perspective. Evol Appl 5:154–167.
629 https://doi.org/10.1111/j.1752-4571.2011.00208.x

630 Varpe Ø (2017) Life history adaptations to seasonality. Integr Comp Biol 57:943–960.
631 https://doi.org/10.1093/icb/icx123

632 Vasconcellos RM, Araújo FG, de Sousa Santos JN, de Araújo Silva M (2011) Diel seasonality in
633 fish biodiversity in a sandy beach in south-eastern Brazil. Marine Biological Association of
634 the United Kingdom 91:1337–1344. https://doi.org/10.1017/S0025315410000652

635 Vihtakari M, Renaud PE, Clarke LJ, et al (2016) Decoding the oxygen isotope signal for
636 seasonal growth patterns in Arctic bivalves. Palaeogeogr Palaeoclimatol Palaeoecol
637 446:263–283. https://doi.org/10.1016/j.palaeo.2016.01.008

638 Warne CPK, McCann KS, Rooney N, et al (2020) Geography and morphology affect the ice
639 duration dynamics of northern hemisphere lakes worldwide. Geophys Res Lett 47:1–10.
640 https://doi.org/10.1029/2020GL087953

641 White ER, Hastings A (2020) Seasonality in ecology: Progress and prospects in theory.
642 Ecological Complexity 44:1–6. https://doi.org/10.1016/j.ecocom.2020.100867

643

644 **Table 1:** Lotka-Volterra Coexistence Conditions vs. Seasonal Coexistence Conditions.

	Lotka – Volterra Criteria	Seasonal Coexistence Criteria
Stable Coexistence	$\alpha_{11} > \alpha_{21}$	$\frac{\mathbf{pr}_{P,1}\alpha_{P,11} + (\mathbf{1}-\mathbf{p})\mathbf{r}_{LP,1}\alpha_{LP,11}}{\mathbf{pr}_{P,1} + (\mathbf{1}-\mathbf{p})\mathbf{r}_{LP,1}} > \frac{\mathbf{pr}_{P,2}\alpha_{P,21} + (\mathbf{1}-\mathbf{p})\mathbf{r}_{LP,2}\alpha_{LP,21}}{\mathbf{pr}_{P,2} + (\mathbf{1}-\mathbf{p})\mathbf{r}_{LP,2}}$
	$\alpha_{22} > \alpha_{12}$	$\frac{\mathbf{pr}_{P,2}\alpha_{P,22} + (\mathbf{1}-\mathbf{p})\mathbf{r}_{LP,2}\alpha_{LP,22}}{\mathbf{pr}_{P,2} + (\mathbf{1}-\mathbf{p})\mathbf{r}_{LP,2}} > \frac{\mathbf{pr}_{P,1}\alpha_{P,12} + (\mathbf{1}-\mathbf{p})\mathbf{r}_{LP,1}\alpha_{LP,12}}{\mathbf{pr}_{P,1} + (\mathbf{1}-\mathbf{p})\mathbf{r}_{LP,1}}$
Competitive Exclusion by sp_1	$\alpha_{11} > \alpha_{21}$	$\frac{\mathbf{pr}_{P,1}\alpha_{P,11} + (\mathbf{1}-\mathbf{p})\mathbf{r}_{LP,1}\alpha_{LP,11}}{\mathbf{pr}_{P,1} + (\mathbf{1}-\mathbf{p})\mathbf{r}_{LP,1}} > \frac{\mathbf{pr}_{P,2}\alpha_{P,21} + (\mathbf{1}-\mathbf{p})\mathbf{r}_{LP,2}\alpha_{LP,21}}{\mathbf{pr}_{P,2} + (\mathbf{1}-\mathbf{p})\mathbf{r}_{LP,2}}$
	$\alpha_{22} < \alpha_{12}$	$\frac{\mathbf{pr}_{P,2}\alpha_{P,22} + (\mathbf{1}-\mathbf{p})\mathbf{r}_{LP,2}\alpha_{LP,22}}{\mathbf{pr}_{P,2} + (\mathbf{1}-\mathbf{p})\mathbf{r}_{LP,2}} < \frac{\mathbf{pr}_{P,1}\alpha_{P,12} + (\mathbf{1}-\mathbf{p})\mathbf{r}_{LP,1}\alpha_{LP,12}}{\mathbf{pr}_{P,1} + (\mathbf{1}-\mathbf{p})\mathbf{r}_{LP,1}}$
Competitive Exclusion by sp_2	$\alpha_{11} > \alpha_{21}$	$\frac{\mathbf{pr}_{P,1}\alpha_{P,11} + (\mathbf{1}-\mathbf{p})\mathbf{r}_{LP,1}\alpha_{LP,11}}{\mathbf{pr}_{P,1} + (\mathbf{1}-\mathbf{p})\mathbf{r}_{LP,1}} > \frac{\mathbf{pr}_{P,2}\alpha_{P,21} + (\mathbf{1}-\mathbf{p})\mathbf{r}_{LP,2}\alpha_{LP,21}}{\mathbf{pr}_{P,2} + (\mathbf{1}-\mathbf{p})\mathbf{r}_{LP,2}}$
	$\alpha_{22} < \alpha_{12}$	$\frac{\mathbf{pr}_{P,2}\alpha_{P,22} + (\mathbf{1}-\mathbf{p})\mathbf{r}_{LP,2}\alpha_{LP,22}}{\mathbf{pr}_{P,2} + (\mathbf{1}-\mathbf{p})\mathbf{r}_{LP,2}} < \frac{\mathbf{pr}_{P,1}\alpha_{P,12} + (\mathbf{1}-\mathbf{p})\mathbf{r}_{LP,1}\alpha_{LP,12}}{\mathbf{pr}_{P,1} + (\mathbf{1}-\mathbf{p})\mathbf{r}_{LP,1}}$
Contingent Coexistence	$\alpha_{11} < \alpha_{21}$	$\frac{\mathbf{pr}_{P,1}\alpha_{P,11} + (\mathbf{1}-\mathbf{p})\mathbf{r}_{LP,1}\alpha_{LP,11}}{\mathbf{pr}_{P,1} + (\mathbf{1}-\mathbf{p})\mathbf{r}_{LP,1}} < \frac{\mathbf{pr}_{P,2}\alpha_{P,21} + (\mathbf{1}-\mathbf{p})\mathbf{r}_{LP,2}\alpha_{LP,21}}{\mathbf{pr}_{P,2} + (\mathbf{1}-\mathbf{p})\mathbf{r}_{LP,2}}$
	$\alpha_{22} < \alpha_{12}$	$\frac{\mathbf{pr}_{P,2}\alpha_{P,22} + (\mathbf{1}-\mathbf{p})\mathbf{r}_{LP,2}\alpha_{LP,22}}{\mathbf{pr}_{P,2} + (\mathbf{1}-\mathbf{p})\mathbf{r}_{LP,2}} < \frac{\mathbf{pr}_{P,1}\alpha_{P,12} + (\mathbf{1}-\mathbf{p})\mathbf{r}_{LP,1}\alpha_{LP,12}}{\mathbf{pr}_{P,1} + (\mathbf{1}-\mathbf{p})\mathbf{r}_{LP,1}}$

645

Figure 1

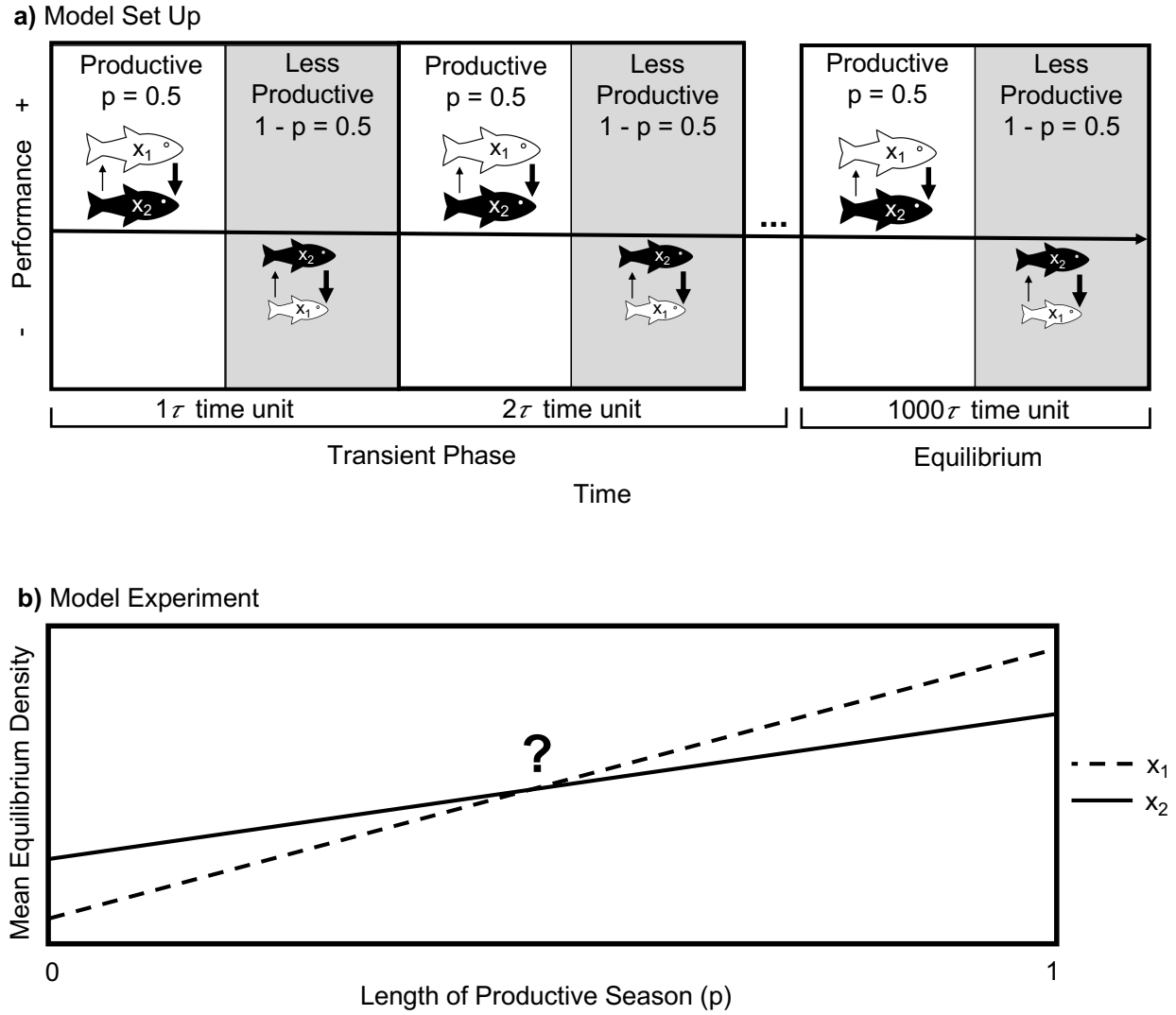

Fig. 1 Model schematic investigates the projected mean equilibrium density over the length of the productive season when species compete under different periodic conditions. a) The model set-up investigates two time-separated seasons with different environmental conditions (productive (white box) and less productive (gray box)). In numerical simulations, competitive species, X_1 (white fish) and X_2 (black fish), exhibit different trade-offs in response to these differing environmental conditions, where each species may experience different levels of inter- to intraspecific competitive interactions (thickness of arrows) depending on which species may have an overall better performance (in terms of growth and competition) in one season compared to the other. An experiment is projected over many periods (say 1000 time-units) of length τ until it reaches an asymptotic state (we refer to this as an equilibrium despite the within-year variation). b) In the model experiment, the projected mean equilibrium density, which represents a fluctuating' species density at its asymptote, is calculated as the duration of the productive season (as a proportion of each time unit) varies from 0 – 1.

Figure 2

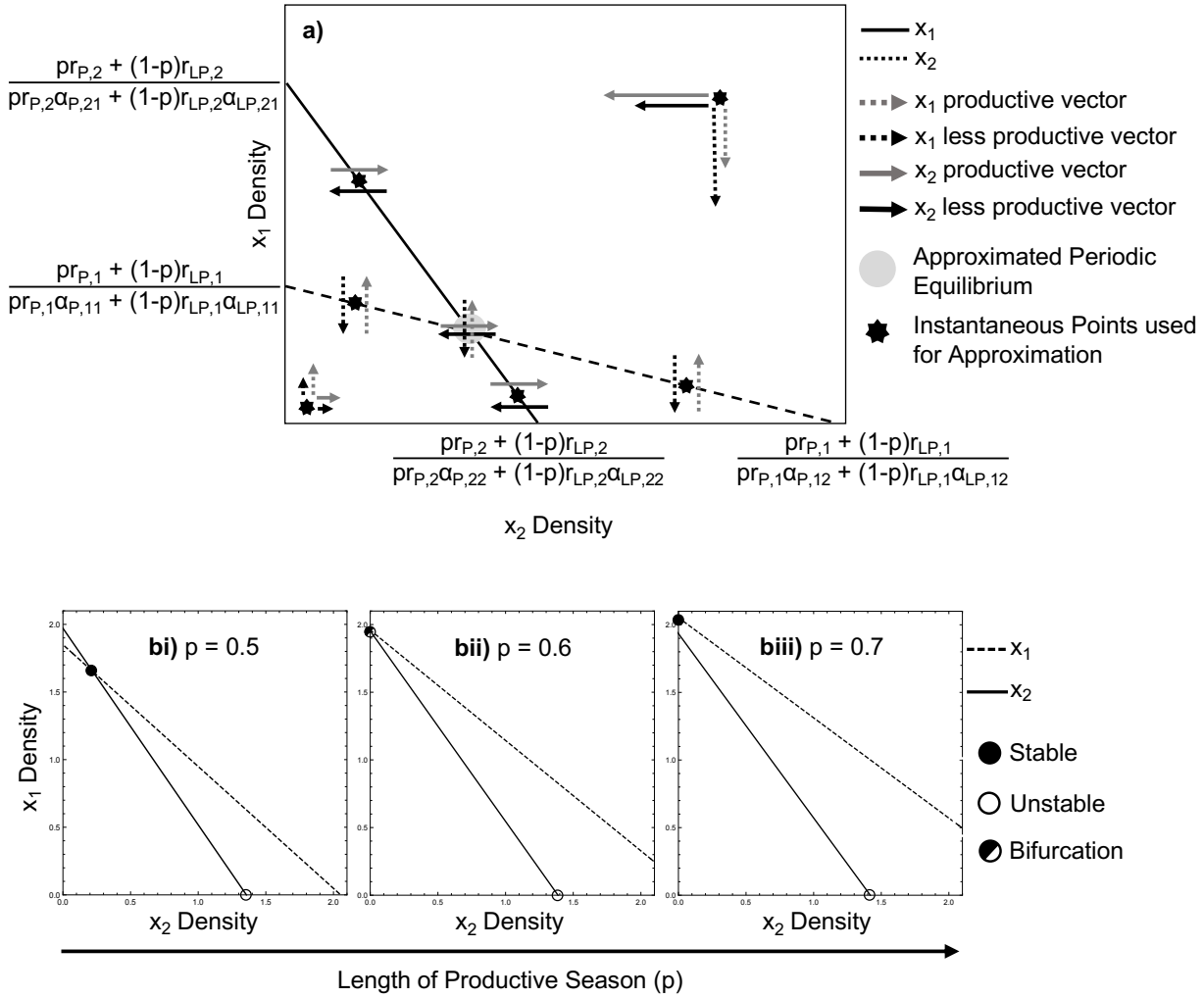

Fig. 2 Isocline approximation of X_1 density on X_2 density. a) Stable coexistence isocline approximation on phaseplane of X_1 (dashed line) and X_2 (solid line) densities. Approximate isocline solutions for a given species occur when the instantaneous rate of change (represented by vector arrows) in each season, scaled by seasonal duration, are equal and opposite of each other (i.e., they "cancel" each other out such that the net change over a full period is null). Refer to Table 1 for similarities to Lotka–Volterra coexistence conditions. b i-iii) illustrates a *p*-driven bifurcation, showing the movement of the isoclines as the productivity season travels from i) p = 0.5; coexistence, to ii) p = 0.6; transcritical bifurcation, to iii) p = 0.7; competitive exclusion of species 2. Parametric values: $\alpha_{P,11}$=0.44, $\alpha_{P,22}$=0.66, $\alpha_{P,12}$=0.25, $\alpha_{P,21}$=0.53, $\alpha_{LP,11}$=1.11, $\alpha_{LP,22}$=0.83, $\alpha_{LP,12}$=1.83, $\alpha_{LP,21}$=0.48, $r_{P,1}$=1.7, $r_{P,2}$=1.2, $r_{LP,1}$=0.3, $r_{LP,2}$=1.

673 **Figure 3**

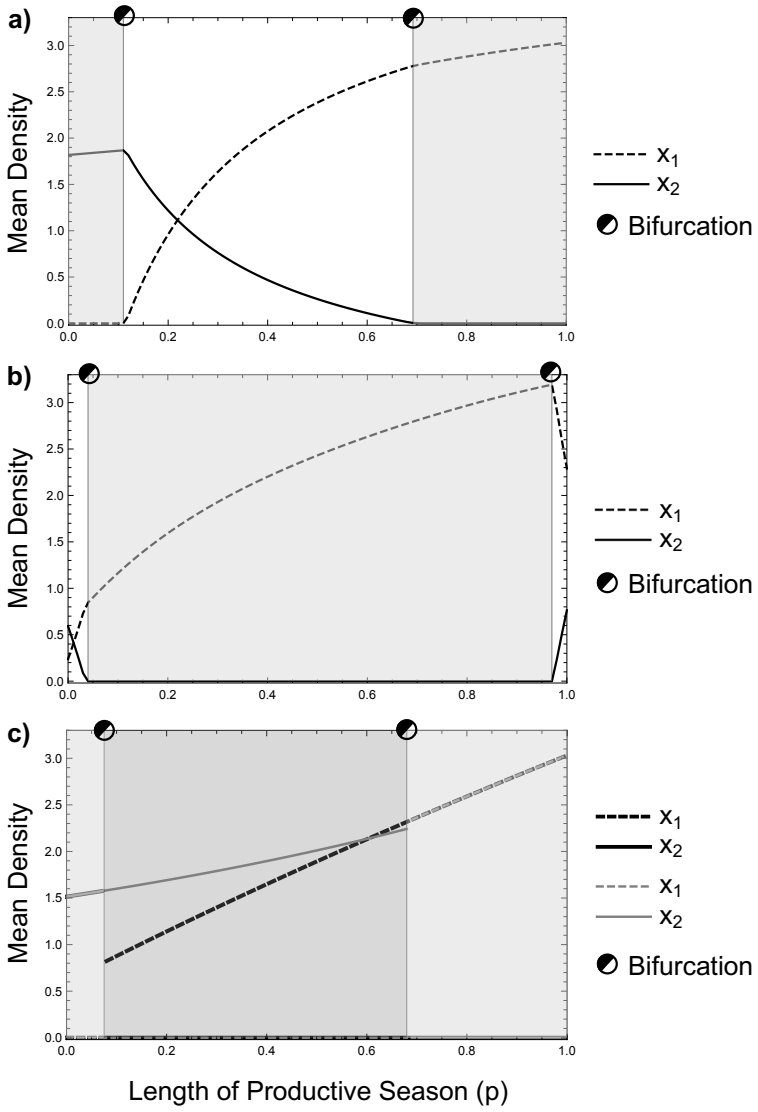

674

675 **Fig. 3** Numerical simulations of mean density over length of productive season (*p*) for
676 seasonally-mediated outcomes. White zone represents stable coexistence, light gray zone
677 represents competitive exclusion, and dark gray zone represents contingent coexistence where
678 the equilibrium is unstable and multiple attractors exist between the two species. a) Seasonally-
679 mediated coexistence. Parametric values: $\alpha_{P,21}$=0.35, $\alpha_{P,12}$=0.165, $\alpha_{P,11}$=0.33, $\alpha_{P,22}$=0.436,
680 $r_{P,1}$=1.7, $r_{P,2}$=1.2, $\alpha_{LP,21}$=0.385, $\alpha_{LP,12}$=0,805, $\alpha_{LP,11}$=0.73, $\alpha_{LP,22}$=0.55, $r_{LP,1}$=0.3, $r_{LP,2}$=1. b)
681 Seasonally-mediated competitive exclusion. Parametric values: $\alpha_{P,21}$=0.29, $\alpha_{P,12}$=0.38,
682 $\alpha_{P,11}$=0.31, $\alpha_{P,22}$=0.44, $r_{P,1}$=4, $r_{P,2}$=1.2, $\alpha_{LP,21}$=1.27, $\alpha_{LP,12}$=1.02, $\alpha_{LP,11}$=1,67, $\alpha_{LP,22}$=1.18 $r_{LP,1}$=0.3,
683 $r_{LP,2}$=1. c) Seasonally-mediated contingent coexistence. Parametric values; $\alpha_{P,21}$=0.548,
684 $\alpha_{P,12}$=0.33, $\alpha_{P,11}$=0.33, $\alpha_{P,22}$=0.363, $r_{P,1}$=1.7, $r_{P,2}$=1.2, $\alpha_{LP,21}$=1.31, $\alpha_{LP,12}$=1.89, $\alpha_{LP,11}$=1.65,
685 $\alpha_{LP,22}$=0.66, $r_{LP,1}$=0.3, $r_{LP,2}$=1.

Figure 4

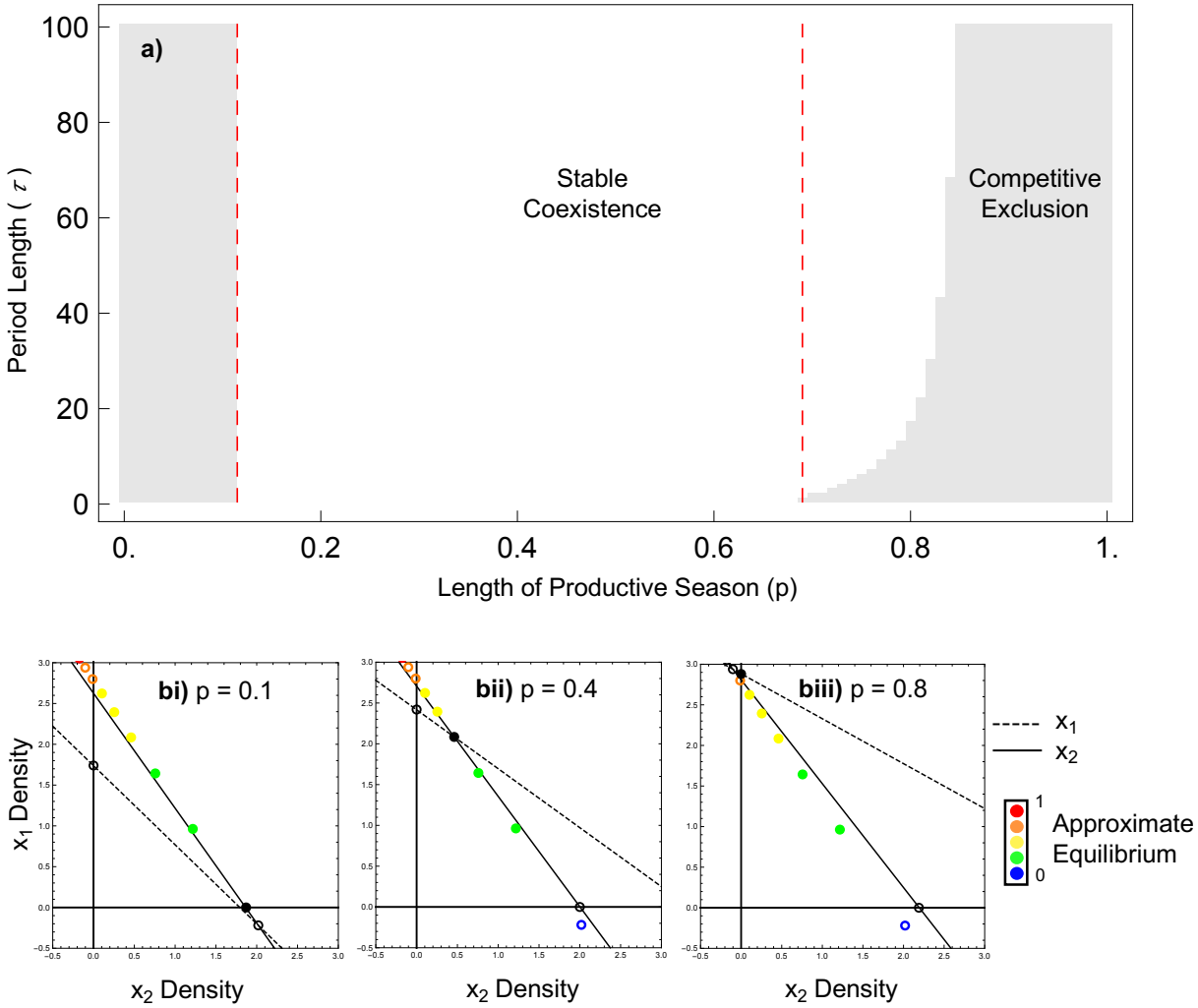

Fig. 4 Two-dimensional bifurcation diagram of seasonally-mediated coexistence**.** a) seasonally-mediated coexistence expanding over a wide range of period lengths (τ). The red dashed lines represent the isocline approximation's prediction of the two transcritical bifurcation points at p=0.115 and p=0.69 (see Fig. S3.1 for complete transition across p, and S4.1 for explanation of approximation accuracy of seasonally mediated coexistence). b) isocline approximation tracks the approximate equilibrium, which represents the mean asymptotic behavior, as the productive season (p) increases from i) p=0.1; competitive exclusion of species 1, to ii) p=0.4; stable coexistence, to iii) p=0.8; competitive exclusion of species 2. Filled in circles are stable equilibrium points, and open circles are unstable equilibrium points. Parametric values: $\alpha_{P,21}$=0.35, $\alpha_{P,12}$=0.165, $\alpha_{P,11}$=0.33, $\alpha_{P,22}$=0.436, $r_{P,1}$=1.7, $r_{P,2}$=1.2, $\alpha_{LP,21}$=0.385, $\alpha_{LP,12}$=0,805, $\alpha_{LP,11}$=0.73, $\alpha_{LP,22}$=0.55, $r_{LP,1}$=0.3, $r_{LP,2}$=1.

Figure 5

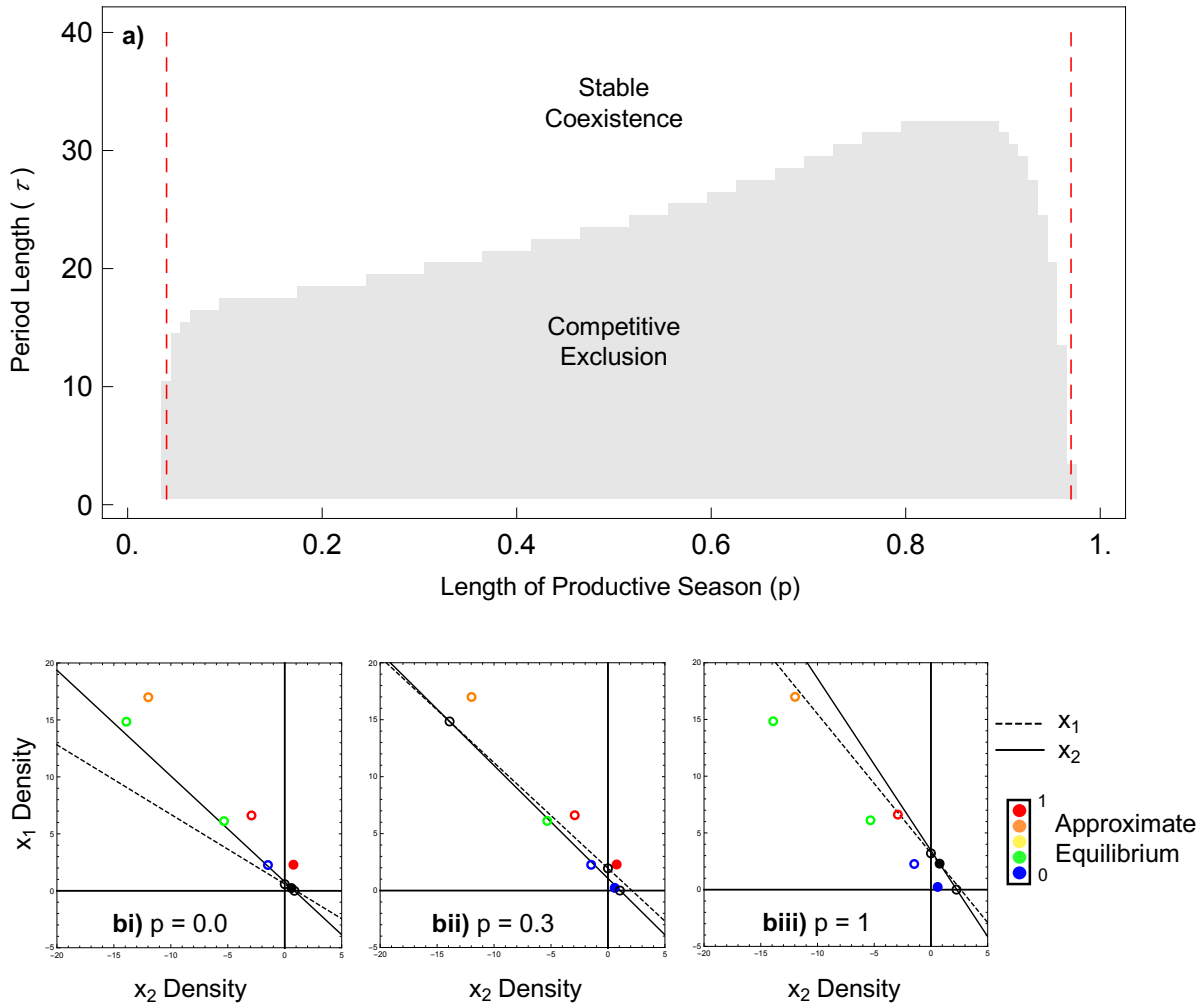

Fig. 5 Two-dimensional bifurcation diagram of seasonally-mediated competitive exclusion. a) seasonally-mediated competitive exclusion expanding over a wide range of period lengths (τ). The red dashed lines represent the isocline approximation's prediction of the two transcritical bifurcation points at p=0.04 and p=0.97 (see Fig. S3.2 for complete transition across p, and S4.2 for explanation of approximation accuracy of seasonally mediated competitive exclusion). b) isocline approximation tracks the approximate equilibrium, which represents the mean asymptotic behaviour, as the productive season increases from i) p=0.0; stable coexistence, to ii) p=0.3; competitive exclusion of species 2, and back to iii) p=1.0; stable coexistence. Filled in circles are stable equilibrium points, and open circles are unstable equilibrium points. Parametric values: $\alpha_{P,21}$=0.29, $\alpha_{P,12}$=0.38, $\alpha_{P,11}$=0.31, $\alpha_{P,22}$=0.44, $r_{P,1}$=4, $r_{P,2}$=1.2, $\alpha_{LP,21}$=1.27, $\alpha_{LP,12}$=1.02, $\alpha_{LP,11}$=1,67, $\alpha_{LP,22}$=1.18 $r_{LP,1}$=0.3, $r_{LP,2}$=1.

Figure 6

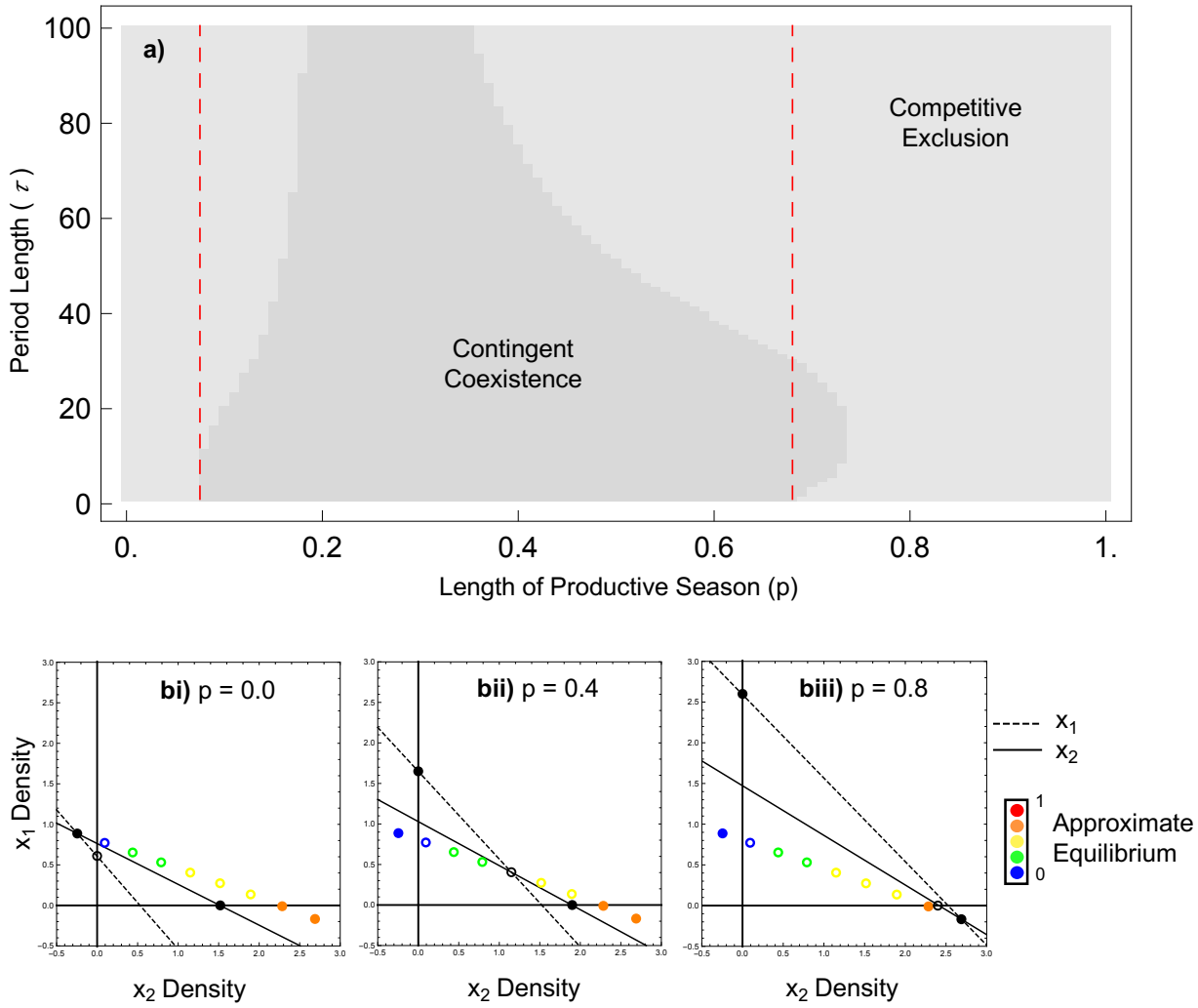

Fig. 6 Two-dimensional bifurcation diagram of seasonally-mediated contingent coexistence. a) seasonally-mediated contingent coexistence expanding over a wide range of period length (τ). The red dashed lines represent the isocline approximation's prediction of the two transcritical bifurcation points at p=0.07 and p=0.69 (see Fig. S3.3 for complete transition across p, and S4.3 for explanation of approximation accuracy of seasonally mediated contingent coexistence). b) isocline approximation tracks the approximate equilibrium, which represents the mean asymptotic behaviour, as the productive season increases from i) p=0.0; competitive exclusion of species 1, to ii) p=0.4; contingent coexistence, to iii) p=0.8; competitive exclusion of species 2. Filled in circles are stable equilibrium points, and open circles are unstable equilibrium points. Parametric values; $\alpha_{P,21}$=0.548, $\alpha_{P,12}$=0.33, $\alpha_{P,11}$=0.33, $\alpha_{P,22}$=0.363, $r_{P,1}$=1.7, $r_{P,2}$=1.2, $\alpha_{LP,21}$=1.31, $\alpha_{LP,12}$=1.89, $\alpha_{LP,11}$=1.65, $\alpha_{LP,22}$=0.66, $r_{LP,1}$=0.3, $r_{LP,2}$=1.

Coexistence in Periodic Environments: Supplementary Material

S1: A Linearization of the Periodic Lotka-Volterra Dynamics

If we consider any point on the phaseplane (X_1-X_2) due to the productive season that lasts from 0 to τp where τ is the period length, and p is the proportion of each period that is considered productive, then we know:

$$X_{P,1}(\tau p) = X_{P,1}(0) + \int_0^{\tau p} \frac{dX_{P,1}}{dt} dt \tag{1}$$

$$X_{P,2}(\tau p) = X_{P,2}(0) + \int_0^{\tau p} \frac{dX_{P,2}}{dt} dt \tag{2}$$

These dynamics follow the differential equation over the trajectory from 0 to τp starting at the values $X_{P,j}(0)$. We linearize the trajectory over 0 to τp by assuming the $\frac{dX_{P,j}}{dt}$ remains constant (e.g., we calculate the instantaneous $\frac{dX_{P,j}}{dt}$ for a point in the phaseplane, say for time (0)). As this is now a constant, we can use the Fundamental Theorem of Calculus to solve for Equations (1) and (2) above yielding:

$$X_{P,1}(\tau p) - X_{P,1}(0) = \frac{dX_{P,1}}{dt}\ t\ \Big|_0^{\tau p} \tag{3}$$

$$X_{P,1}(\tau p) - X_{P,1}(0) = \tau p \frac{dX_{P,1}}{dt} - 0\frac{dX_{P,1}}{dt} \tag{4}$$

$$X_{P,1}(\tau p) - X_{P,1}(0) = \tau p \frac{dX_{P,1}}{dt} \tag{5}$$

Similarly, we solve for the less productive season between τp and τ, giving us:

$$X_{LP,1}(\tau) - X_{LP,1}(\tau p) = \tau(1-p)\frac{dX_{LP,1}}{dt} \tag{6}$$

737 Thus, the linearization estimates the trajectory as a linear scale movement following the length of
738 the time interval (either τp, or $\tau(1-p)$). We can take this simple estimate to estimate the within
739 seasonal dynamics and use them to estimate the periodic 0-isoclines.

740

741 Given Equations (5) and (6), the X_1 isocline occurs when:

$$\tau p\frac{dX_{P,1}}{dt} = -\tau(1-p)\frac{dX_{LP,1}}{dt} \tag{7}$$

742

743 With this approximation, we substitute the productive and less productive Lotka-Volterra models
744 into equation (7):

$$\tau p\, r_{P,1}X_1(1-\alpha_{P,11}X_1-\alpha_{P,12}X_2) = -\tau(1-p)\, r_{LP,1}X_1(1-\alpha_{LP,11}X_1-\alpha_{LP,12}X_2) \tag{8}$$

745

746 Noticing that τ cancels out, we can now solve for the isocline solution:

$$X_1 = -\frac{pr_{P,1}\alpha_{P,12}+(1-p)r_{LP,1}\alpha_{LP,12}}{pr_{P,1}\alpha_{P,11}+(1-p)r_{LP,1}\alpha_{LP,11}}X_2 + \frac{pr_{P,1}+(1-p)r_{LP,1}}{pr_{P,1}\alpha_{P,11}+(1-p)r_{LP,1}\alpha_{LP,11}} \tag{9}$$

747

748 Similarly, we would perform the same steps to find the isocline solution for X_2. This isocline
749 approximation, for both species, allows us to determine coexistence criteria for seasonal
750 environments.

S2: Isocline Approximation and Numerical Simulation Comparison

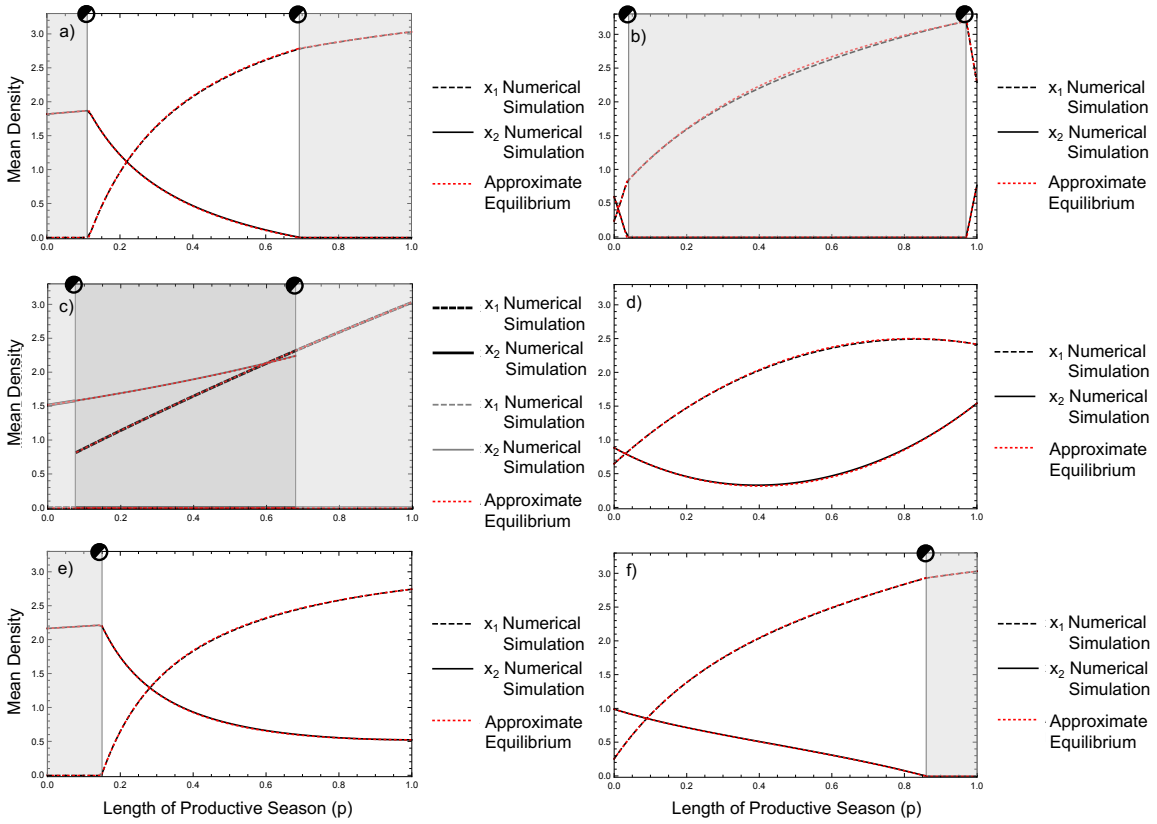

Fig. S2.1 Comparison of Isocline Approximation against Numerical Simulations. White zone represents stable coexistence, light gray zone represents competitive exclusion, and dark gray zone represents contingent coexistence. a) Seasonally mediated coexistence. Parametric values: $\alpha_{P,21}$=0.35, $\alpha_{P,12}$=0.165, $\alpha_{P,11}$=0.33, $\alpha_{P,22}$=0.436, $r_{P,1}$=1.7, $r_{P,2}$=1.2, $\alpha_{LP,21}$=0.385, $\alpha_{LP,12}$=0,805, $\alpha_{LP,11}$=0.73, $\alpha_{LP,22}$=0.55, $r_{LP,1}$=0.3, $r_{LP,2}$=1. b) Seasonally mediated competitive exclusion. Parametric values: $\alpha_{P,21}$=0.29, $\alpha_{P,12}$=0.38, $\alpha_{P,11}$=0.31, $\alpha_{P,22}$=0.44, $r_{P,1}$=4, $r_{P,2}$=1.2, $\alpha_{LP,21}$=1.27, $\alpha_{LP,12}$=1.02, $\alpha_{LP,11}$=1,67, $\alpha_{LP,22}$=1.18 $r_{LP,1}$=0.3, $r_{LP,2}$=1. c) Seasonally mediated contingent coexistence. The equilibrium is unstable in the dark gray zone and multiple attractors exist between the two species. Parametric values: $\alpha_{P,21}$=0.548, $\alpha_{P,12}$=0.33, $\alpha_{P,11}$=0.33, $\alpha_{P,22}$=0.363, $r_{P,1}$=1.7, $r_{P,2}$=1.2, $\alpha_{LP,21}$=1.31, $\alpha_{LP,12}$=1.89, $\alpha_{LP,11}$=1.65, $\alpha_{LP,22}$=0.66, $r_{LP,1}$=0.3, $r_{LP,2}$=1. d) Counterintuitive mean density change. Parametric values: $\alpha_{P,21}$=0.2, $\alpha_{P,12}$=0.155, $\alpha_{P,11}$=0.315, $\alpha_{P,22}$=0.335, $r_{P,1}$=1.7, $r_{P,2}$=1.2, $\alpha_{LP,21}$=0.57, $\alpha_{LP,12}$=0.4, $\alpha_{LP,11}$=1, $\alpha_{LP,22}$=0.715, $r_{LP,1}$=0.3, $r_{LP,2}$=1. e) Mean density changes with competitive exclusion in the less productive season. Parametric values: $\alpha_{P,21}$=0.288, $\alpha_{P,12}$=0.15, $\alpha_{P,11}$=0.336, $\alpha_{P,22}$=0.402, $r_{P,1}$=1.7, $r_{P,2}$=1.2, $\alpha_{LP,21}$=0.354, $\alpha_{LP,12}$=0.75, $\alpha_{LP,11}$=0.666, $\alpha_{LP,22}$=0.462, $r_{LP,1}$=0.3, $r_{LP,2}$=1. f) Mean density changes with competitive exclusion in the productive season. Parametric values: $\alpha_{P,21}$=0.35, $\alpha_{P,12}$=0.165, $\alpha_{P,11}$=0.33, $\alpha_{P,22}$=0.44, $r_{P,1}$=1.7, $r_{P,2}$=1.2, $\alpha_{LP,21}$=0.28, $\alpha_{LP,12}$=0.825, $\alpha_{LP,11}$=0.73, $\alpha_{LP,22}$=0.94, $r_{LP,1}$=0.3, $r_{LP,2}$=1.

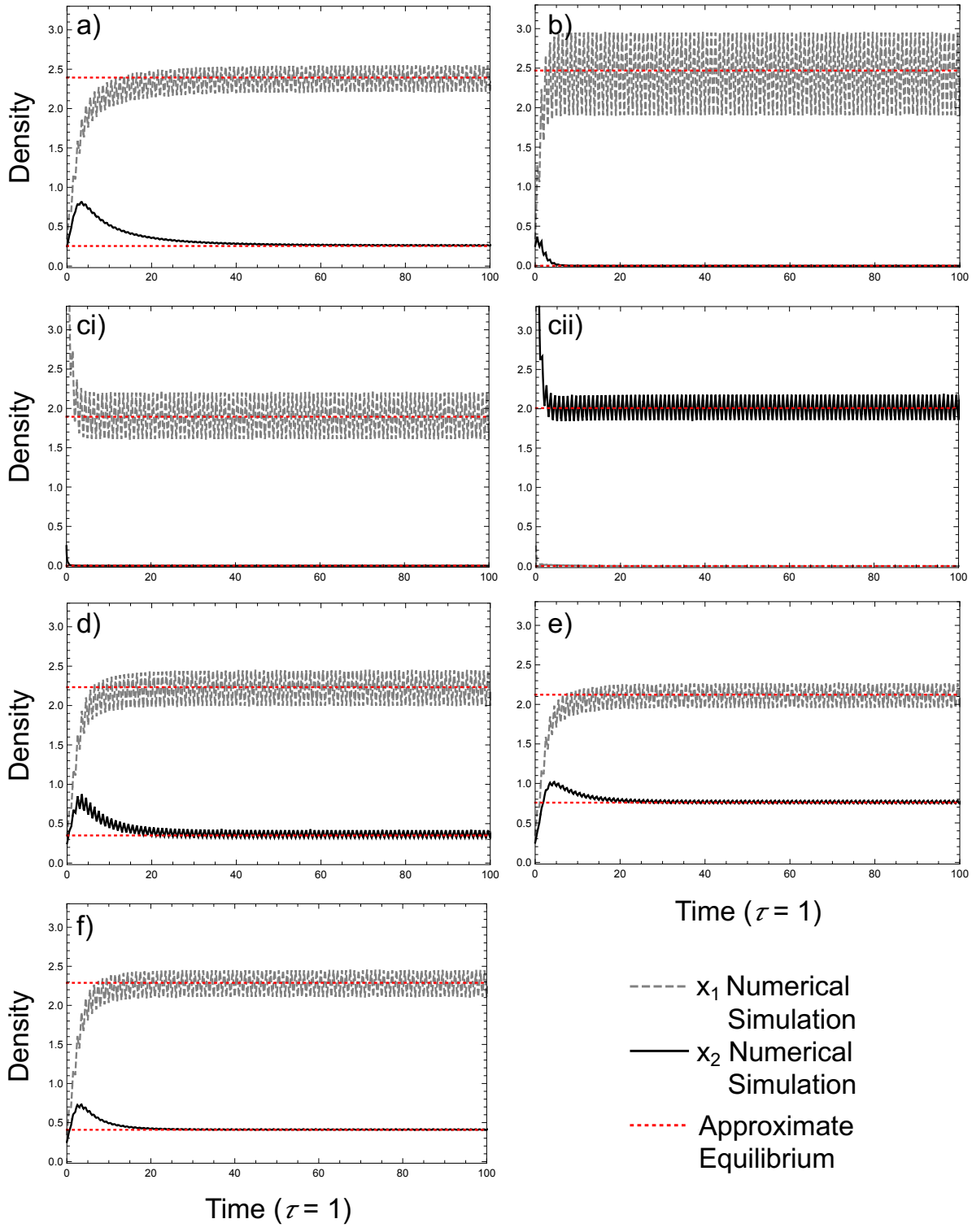

771

772 **Fig. S2.2** Time Series at $p = 0.5$, and $\tau = 1$ for the comparison of isocline approximation against
773 numerical simulations. a) Seasonally mediated coexistence. Parametric values: $\alpha_{P,21}$=0.35,
774 $\alpha_{P,12}$=0.165, $\alpha_{P,11}$=0.33, $\alpha_{P,22}$=0.436, $r_{P,1}$=1.7, $r_{P,2}$=1.2, $\alpha_{LP,21}$=0.385, $\alpha_{LP,12}$=0,805, $\alpha_{LP,11}$=0.73,

$\alpha_{LP,22}$=0.55, $r_{LP,1}$=0.3, $r_{LP,2}$=1. b) Seasonally mediated competitive exclusion. Parametric values: $\alpha_{P,21}$=0.29, $\alpha_{P,12}$=0.38, $\alpha_{P,11}$=0.31, $\alpha_{P,22}$=0.44, $r_{P,1}$=4, $r_{P,2}$=1.2, $\alpha_{LP,21}$=1.27, $\alpha_{LP,12}$=1.02, $\alpha_{LP,11}$=1,67, $\alpha_{LP,22}$=1.18 $r_{LP,1}$=0.3, $r_{LP,2}$=1. ci) Seasonally mediated contingent coexistence. X_1 competitively excluded X_2. Parametric values: $\alpha_{P,21}$=0.548, $\alpha_{P,12}$=0.33, $\alpha_{P,11}$=0.33, $\alpha_{P,22}$=0.363, $r_{P,1}$=1.7, $r_{P,2}$=1.2, $\alpha_{LP,21}$=1.31, $\alpha_{LP,12}$=1.89, $\alpha_{LP,11}$=1.65, $\alpha_{LP,22}$=0.66, $r_{LP,1}$=0.3, $r_{LP,2}$=1. cii) Seasonally mediated contingent coexistence. X_2 competitively excluded X_1. Parametric values: $\alpha_{P,21}$=0.548, $\alpha_{P,12}$=0.33, $\alpha_{P,11}$=0.33, $\alpha_{P,22}$=0.363, $r_{P,1}$=1.7, $r_{P,2}$=1.2, $\alpha_{LP,21}$=1.31, $\alpha_{LP,12}$=1.89, $\alpha_{LP,11}$=1.65, $\alpha_{LP,22}$=0.66, $r_{LP,1}$=0.3, $r_{LP,2}$=1. d) Counterintuitive mean density change. Parametric values: $\alpha_{P,21}$=0.2, $\alpha_{P,12}$=0.155, $\alpha_{P,11}$=0.315, $\alpha_{P,22}$=0.335, $r_{P,1}$=1.7, $r_{P,2}$=1.2, $\alpha_{LP,21}$=0.57, $\alpha_{LP,12}$=0.4, $\alpha_{LP,11}$=1, $\alpha_{LP,22}$=0.715, $r_{LP,1}$=0.3, $r_{LP,2}$=1. e) Mean density changes with competitive exclusion in the less productive season. Parametric values: $\alpha_{P,21}$=0.288, $\alpha_{P,12}$=0.15, $\alpha_{P,11}$=0.336, $\alpha_{P,22}$=0.402, $r_{P,1}$=1.7, $r_{P,2}$=1.2, $\alpha_{LP,21}$=0.354, $\alpha_{LP,12}$=0.75, $\alpha_{LP,11}$=0.666, $\alpha_{LP,22}$=0.462, $r_{LP,1}$=0.3, $r_{LP,2}$=1. f) Mean density changes with competitive exclusion in the productive season. Parametric values: $\alpha_{P,21}$=0.35, $\alpha_{P,12}$=0.165, $\alpha_{P,11}$=0.33, $\alpha_{P,22}$=0.44, $r_{P,1}$=1.7, $r_{P,2}$=1.2, $\alpha_{LP,21}$=0.28, $\alpha_{LP,12}$=0.825, $\alpha_{LP,11}$=0.73, $\alpha_{LP,22}$=0.94, $r_{LP,1}$=0.3, $r_{LP,2}$=1.

S3: Tracking Isocline Approximation across Productivity Length for all Seasonally Mediated Competitive Outcomes

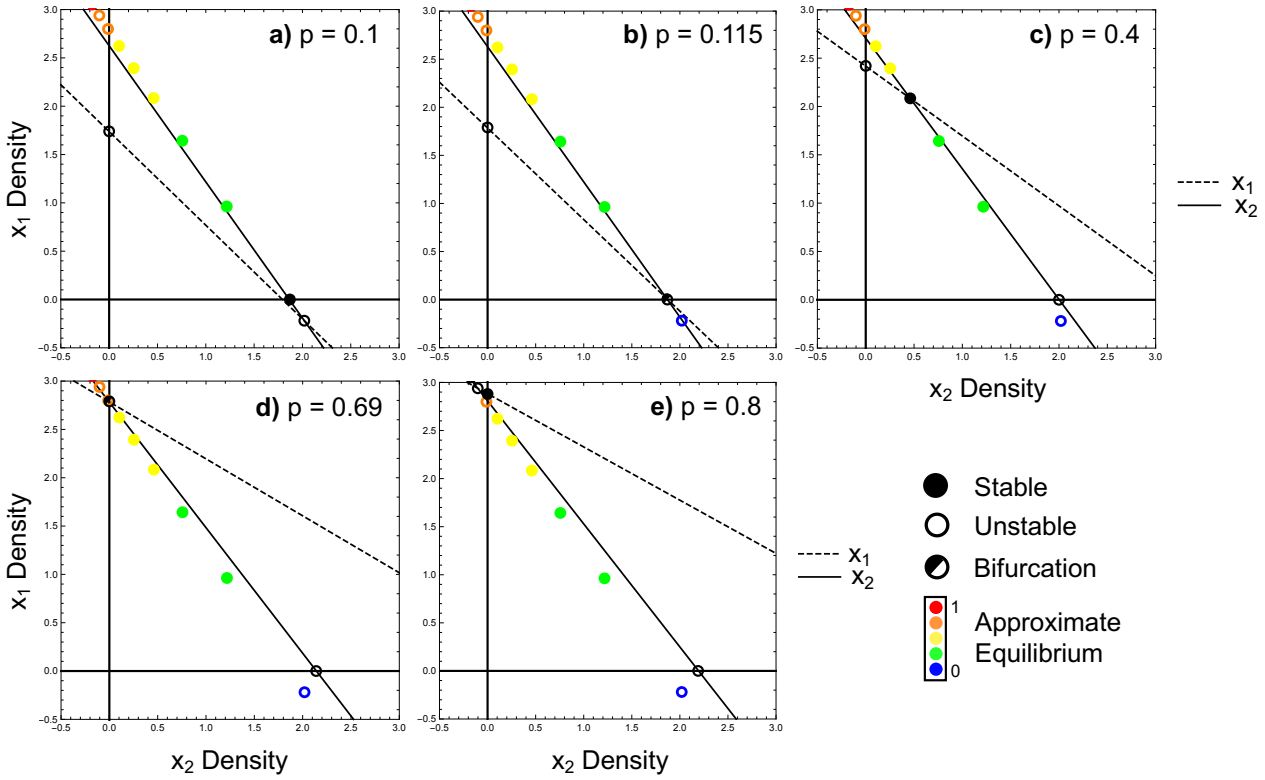

Fig. S3.1 Seasonally mediated coexistence isocline approximation. Isocline approximation tracking the interior equilibrium as the productive season increases in length from a) p=0.1; competitive exclusion of species 1, to b) p=0.115; transcritical bifurcation, to c) p=0.4; stable coexistence, to d) p=0.69; transcritical bifurcation, to e) p=0.8; competitive exclusion of species 2. Parametric values: $\alpha_{P,21}$=0.35, $\alpha_{P,12}$=0.165, $\alpha_{P,11}$=0.33, $\alpha_{P,22}$=0.436, $r_{P,1}$=1.7, $r_{P,2}$=1.2, $\alpha_{LP,21}$=0.385, $\alpha_{LP,12}$=0,805, $\alpha_{LP,11}$=0.73, $\alpha_{LP,22}$=0.55, $r_{LP,1}$=0.3, $r_{LP,2}$=1.

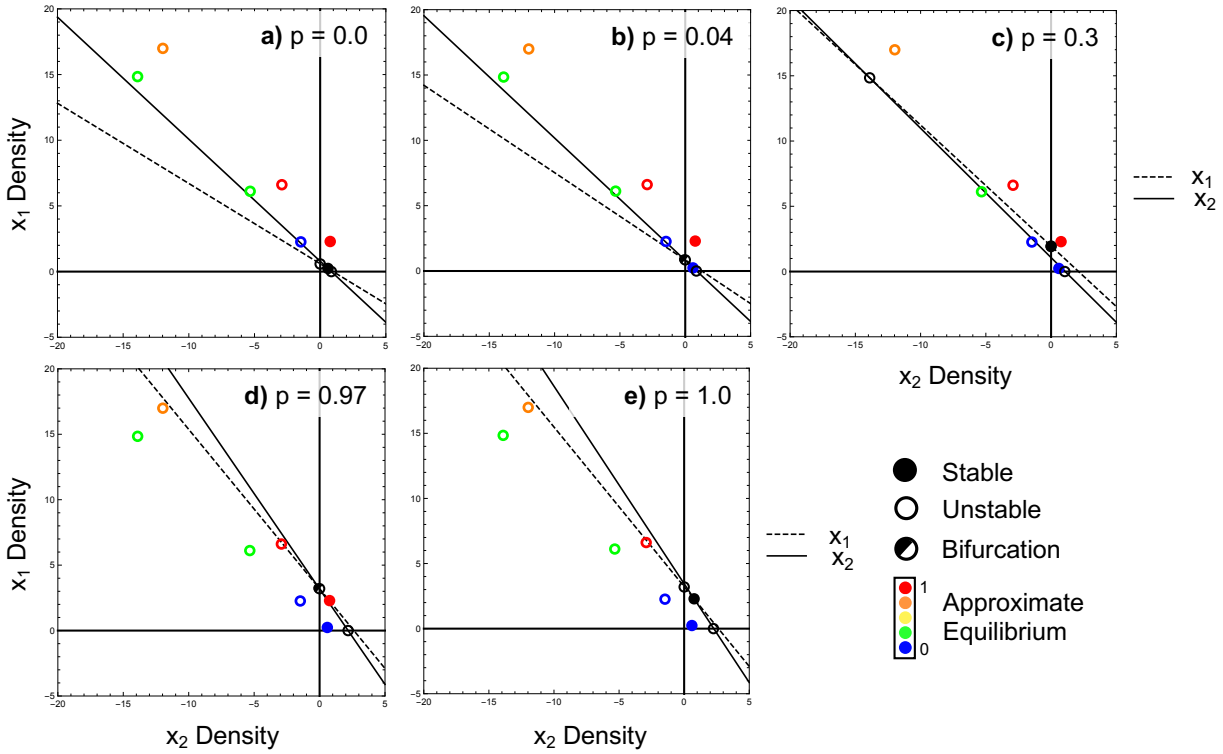

Fig. S3.2 Seasonally mediated competitive exclusion isocline approximation. Isocline approximation tracking the interior equilibrium as the productive season increases in length from a) p=0.0; stable coexistence, to b) p=0.04; transcritical bifurcation, to c) p=0.3; competitive exclusion of species 2, to d) p=0.97; transcritical bifurcation, to e) p=1.0; stable coexistence. Parametric values: $\alpha_{P,21}$=0.29, $\alpha_{P,12}$=0.38, $\alpha_{P,11}$=0.31, $\alpha_{P,22}$=0.44, $r_{P,1}$=4, $r_{P,2}$=1.2, $\alpha_{LP,21}$=1.27, $\alpha_{LP,12}$=1.02, $\alpha_{LP,11}$=1,67, $\alpha_{LP,22}$=1.18 $r_{LP,1}$=0.3, $r_{LP,2}$=1.

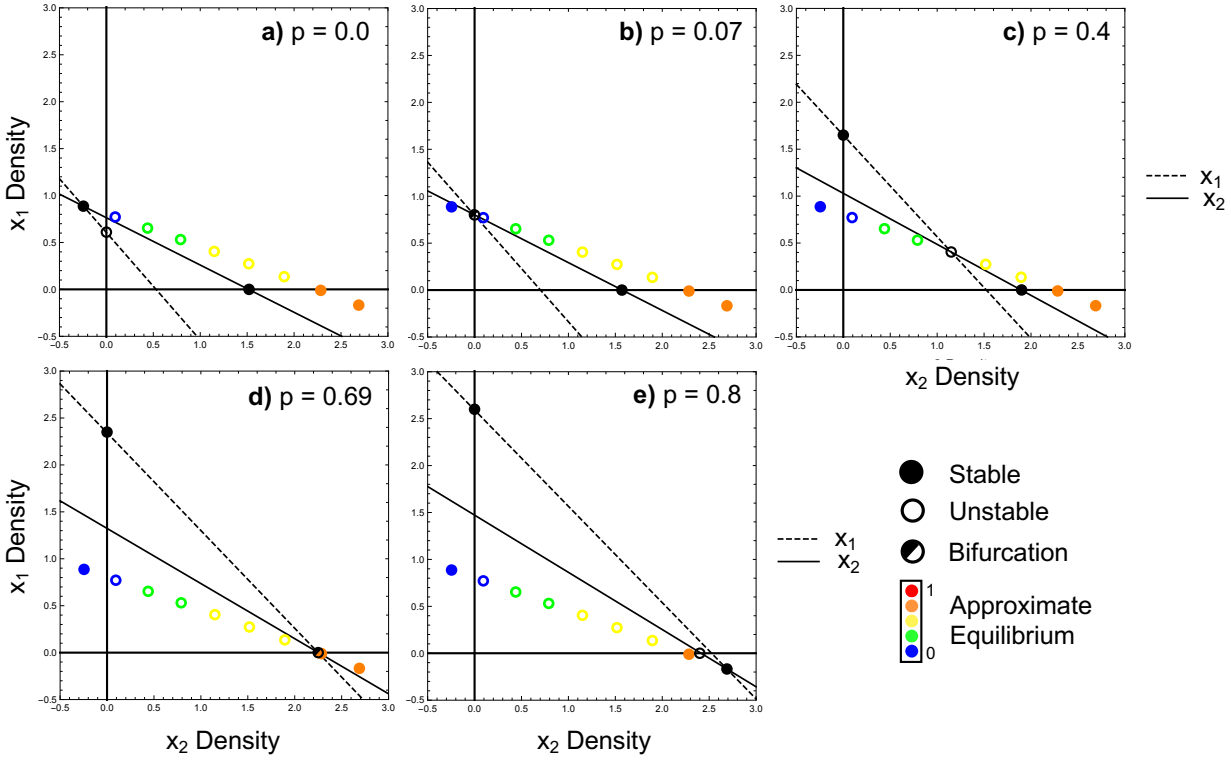

Fig. S3.3 Seasonally mediated contingent coexistence isocline approximation. Isocline approximation tracking the interior equilibrium as the productive season increases in length from a) p=0.0; competitive exclusion of species 1, to b) p=0.07; transcritical bifurcation, to c) p=0.4; contingent coexistence, to d) p=0.69; transcritical bifurcation, to e) p=0.8; competitive exclusion of species 2. Parametric values: $\alpha_{P,21}$=0.548, $\alpha_{P,12}$=0.33, $\alpha_{P,11}$=0.33, $\alpha_{P,22}$=0.363, $r_{P,1}$=1.7, $r_{P,2}$=1.2, $\alpha_{LP,21}$=1.31, $\alpha_{LP,12}$=1.89, $\alpha_{LP,11}$=1.65, $\alpha_{LP,22}$=0.66, $r_{LP,1}$=0.3, $r_{LP,2}$=1.

S4: Accuracy of the Linear Isocline Approximation

Our results hold for a broad range of period lengths but clearly depend on specific parameterizations that alter the timescale or the effects of timescale. Recall that our approximation operates by assuming a zero population growth rate exists in the phaseplane where linearization's of the Lotka-Volterra equations cancel out over the high growth and low growth periods (i.e., linearization of the high growth for species X_1 and species X_2 are both equal and opposite in sign to the low growth linearization). Given this assumption, we can immediately ask when we expect nonlinear dynamics to dominate and potentially threaten the validity of the linear assumption. First, the longer the period of the forced parameters (τ), then the longer the time the dynamics have to fall off the linear assumption. Further, the larger the growth rates (r), the larger the potential for nonlinear dynamics even with smaller periods (τ). As a result, we can say the larger the product $r\tau$, the more likely our assumption of linearity is threatened. Effectively, τr sets the relative pace of the seasonal dynamics.

Recognizing that linear assumptions will lose accuracy when dynamics become nonlinear with longer periods and fast growth rates (i.e., there is more time for dynamics to become nonlinear), we first compare the dynamics (set by the original growth rates in the manuscript) with the approximation's accuracy when the period length (τ) is increased. Next, we slow the dynamics by dividing all species' growth rates (r) by 10-units and compare the approximation's accuracy with these dynamics when the period length increases. Our results below show that indeed our approximation can fall off, but even here for large, combined values of $r\tau$, the approximation remains a reasonable qualitative predictor of steady state behaviour for seasonally-mediated

835 coexistence and contingent coexistent (S4.1 and S4.3 respectively). We note that the seasonally
836 mediated competitive exclusion is not as robust (S4.2).
837
838 As seen in Fig. 4a, the analytical approximation still accurately predicts the numerically
839 generated transcritical bifurcation at $p = 0.11$ (mean densities transition between competitive
840 exclusion of species 1 to coexistence of both species), even when the period length (τ), reaches
841 100 time-units. This is due to the large difference between the productive and less-productive
842 growth rates of species 1. However, the approximation begins to inaccurately predict where the
843 second numerically generated transcritical bifurcation will occur ($p = 0.69$; mean density
844 transition between coexistence and competitive exclusion of species 2) when $\tau = 5$ time-units
845 (Fig. S4.11b). With the original growth rates used in the manuscript, when the period length is
846 small ($\tau = 1$), the seasonal dynamics are relatively linear, and the approximation accurately
847 predict the true mean densities from the numerical simulation (Figs. S4.11a and S4.12a).
848 However, as we increase the period length to 5 time-units, the dynamics become more nonlinear
849 as, with enough time, species' densities reach their seasonal equilibrium and spend more time at
850 these fixed points (Fig. S4.12b). Here, the numerically generated mean densities will be skewed
851 closer towards this equilibrium, while the linear approximation fails to capture this (Fig. S4.11b).
852 When all growth rates are slowed down (all r's divided by 10 units), the seasonal dynamics
853 become more linear, and the approximation is more accurately able to track the mean densities
854 even when the period length (τ) is increased from 1 (Figs S4.11c and S4.12c) to 5 time-units
855 (Figs S4.11d and S4.12d).
856

In Fig. 5a, the approximation still predicts seasonally mediated competitive exclusion, even when species coexist at very large period lengths ($\tau > 33$ time units) across all p-values. However, when τ is increased from 1 to 10 time-units with the original growth rates, the dynamics become more nonlinear (Figs. S4.22a and S4.22b respectively) and the approximation begins to fail at tracking the numerically-generated mean densities throughout the entire range of p-values (Figs. S4.21a and S4.21b respectively), though it still captures the qualitative behavior and presence of the bifurcations. When growth rates are smaller, the seasonal dynamics are now more linear (Figs. S4.22c and FigsS4.22d), and the approximation more accurately tracks the numerically generated mean densities as τ increases from 1 to 10 time-units (Figs. S4.22c and FigsS4.22d respectively).

For seasonally mediated contingent coexistence, as the period length (τ) increases, the region of contingent coexistence from the numerically-generated results first broadens and then shrinks (Fig. 6a). With the original growth rates, as the period length is increased from 1 to 20 time-units, the seasonal dynamics become more nonlinear (Figs. S4.32a and S4.32b respectively), and the approximation is unable to track the true bifurcations based on our numerical results (Figs. S4.31a and S4.31b respectively). When the growth rates are a tenth of their original size (all r's divided by 10 units), the dynamics slow down and are now more linear as τ is increased (Figs. S4.32c and S4.32d), allowing the approximation to more accurately track the numerically-generated mean densities over the entire range of p-values (Figs. S4.31c and S4.31d).

S4.1 Approximation Accuracy of Seasonally Mediated Coexistence

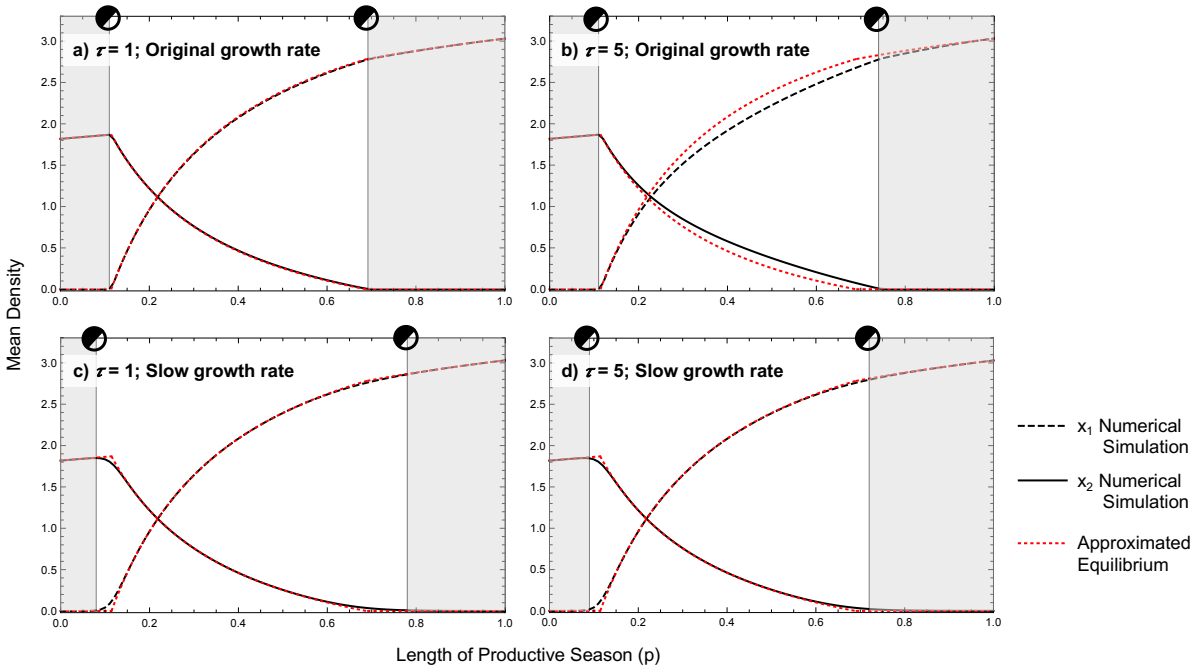

Fig. S4.11 Isocline approximation – mean density plots over the length of the productive season (p) for seasonally-mediated coexistence. White zones represent coexistence and light grey zones represent competitive exclusion. a) and b) original growth rates (those used throughout manuscript: $r_{P1} = 1.7$, $r_{P2} = 1.2$, $r_{LP1} = 1$, $r_{LP2} = 0.3$) when the period length $\tau = 1$ and 5 time-units respectively. c) and d) all growth rates have been divided by 10 units ($r_{P1} = 0.17$, $r_{P2} = 0.12$, $r_{LP1} = 0.1$, $r_{LP2} = 0.03$) when the period length = 1 and 5 time-units respectively. Parametric values: $\alpha_{P,21}$=0.35, $\alpha_{P,12}$=0.165, $\alpha_{P,11}$=0.33, $\alpha_{P,22}$=0.436, $\alpha_{LP,21}$=0.385, $\alpha_{LP,12}$=0,805, $\alpha_{LP,11}$=0.73, $\alpha_{LP,22}$=0.55.

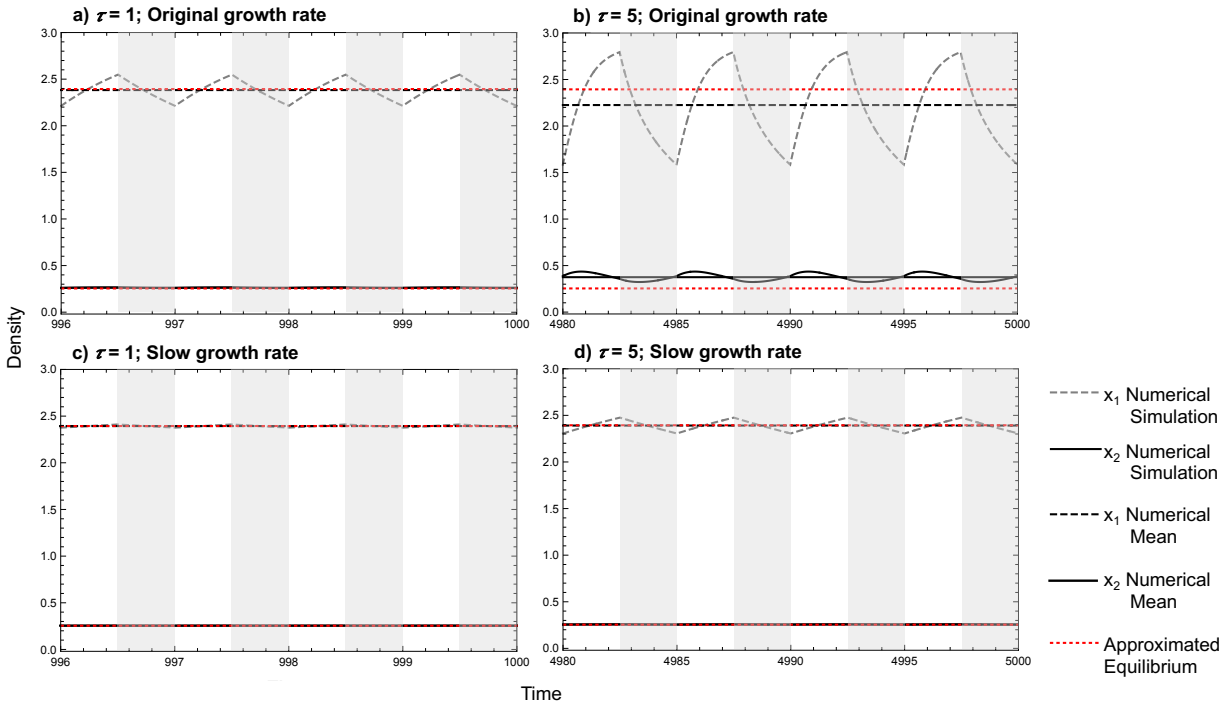

887

888 **Fig. S4.12** Isocline approximation – time series for seasonally-mediated coexistence. Length of
889 productive season (p) = 0.5 represented by white zones, and light grey zones represent the less-
890 productive season. a) and b) original growth rates (those used throughout manuscript: r_{P1} = 1.7,
891 r_{P2} = 1.2, r_{LP1} = 1, r_{LP2} = 0.3) when the period length τ = 1 and 5 time-units respectively. c) and
892 d) all growth rates have been divided by 10 units (r_{P1} = 0.17, r_{P2} = 0.12, r_{LP1} = 0.1, r_{LP2} = 0.03)
893 when the period length = 1 and 5 time-units respectively. Parametric values: $\alpha_{P,21}$=0.35,
894 $\alpha_{P,12}$=0.165, $\alpha_{P,11}$=0.33, $\alpha_{P,22}$=0.436, $\alpha_{LP,21}$=0.385, $\alpha_{LP,12}$=0,805, $\alpha_{LP,11}$=0.73, $\alpha_{LP,22}$=0.55.

S4.2 Approximation Accuracy of Seasonally Mediated Competitive Exclusion

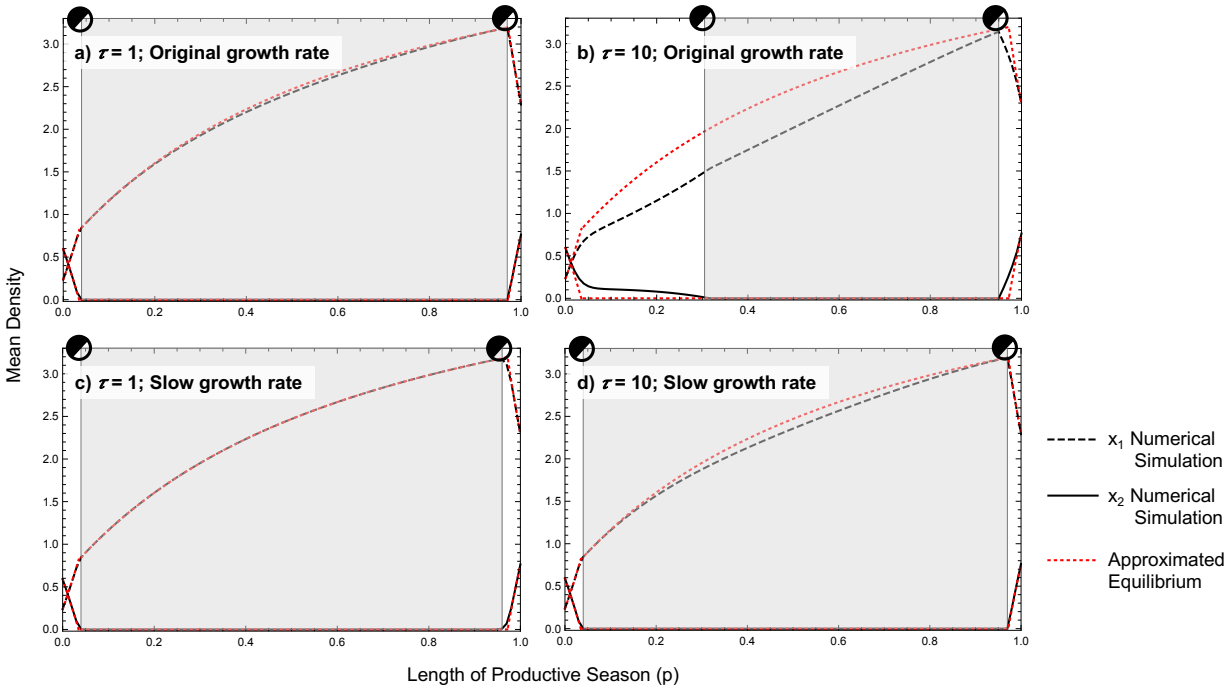

Fig. S4.21 Isocline approximation – mean density plots over the length of the productive season (p) for seasonally-mediated competitive exclusion. White zones represent coexistence and light grey zones represent competitive exclusion. a) and b) original growth rates (those used throughout manuscript: $r_{P1} = 4$, $r_{P2} = 1.2$, $r_{LP1} = 1$, $r_{LP2} = 0.3$) when the period length $\tau = 1$ and 10 time-units respectively. c) and d) all growth rates have been divided by 10 units ($r_{P1} = 0.4$, $r_{P2} = 0.12$, $r_{LP1} = 0.1$, $r_{LP2} = 0.03$) when the period length = 1 and 10 time-units respectively. Parametric values: $\alpha_{P,21}$=0.29, $\alpha_{P,12}$=0.38, $\alpha_{P,11}$=0.31, $\alpha_{P,22}$=0.44, $\alpha_{LP,21}$=1.27, $\alpha_{LP,12}$=1.02, $\alpha_{LP,11}$=1,67, $\alpha_{LP,22}$=1.18.

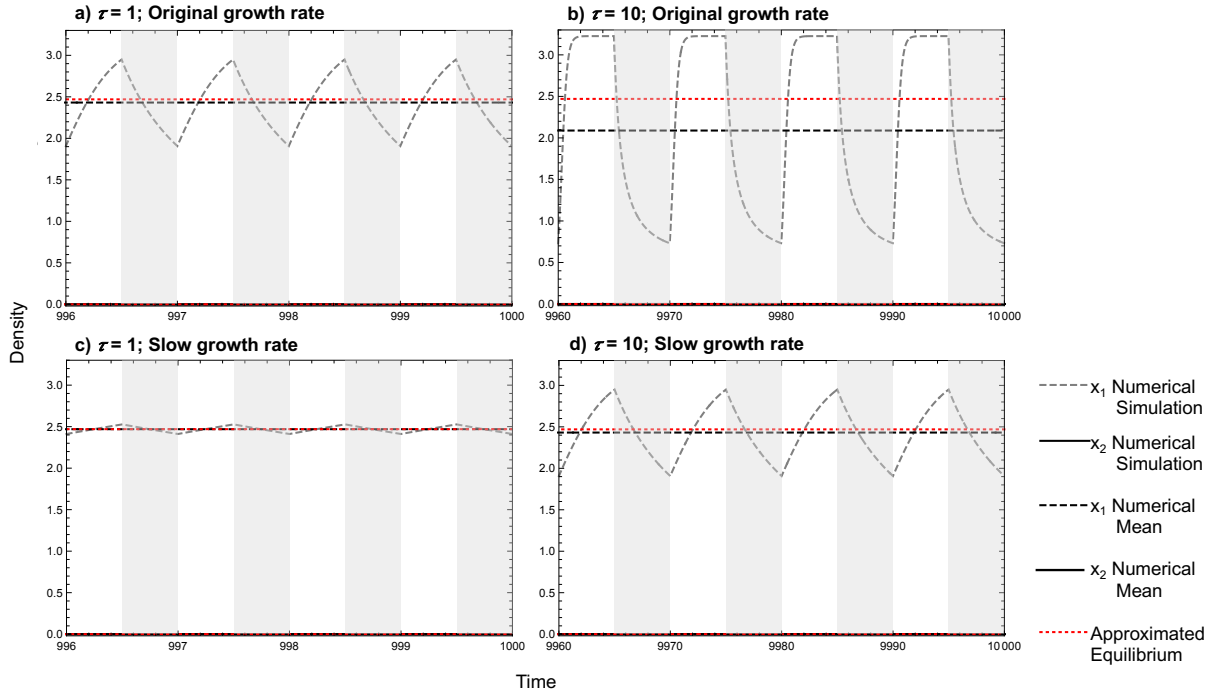

Fig. S4.22 Isocline approximation – time series for seasonally-mediated competitive exclusion. Length of productive season (p) = 0.5 represented by white zones, and light grey zones represent the less-productive season. a) and b) original growth rates (those used throughout manuscript: r_{P1} = 4, r_{P2} = 1.2, r_{LP1} = 1, r_{LP2} = 0.3) when the period length τ = 1 and 10 time-units respectively. c) and d) all growth rates have been divided by 10 units (r_{P1} = 0.4, r_{P2} = 0.12, r_{LP1} = 0.1, r_{LP2} = 0.03) when the period length = 1 and 10 time-units respectively. Parametric values: $\alpha_{P,21}$=0.29, $\alpha_{P,12}$=0.38, $\alpha_{P,11}$=0.31, $\alpha_{P,22}$=0.44, $\alpha_{LP,21}$=1.27, $\alpha_{LP,12}$=1.02, $\alpha_{LP,11}$=1,67, $\alpha_{LP,22}$=1.18.

S4.3 Approximation Accuracy of Seasonally Mediated Contingent Coexistence

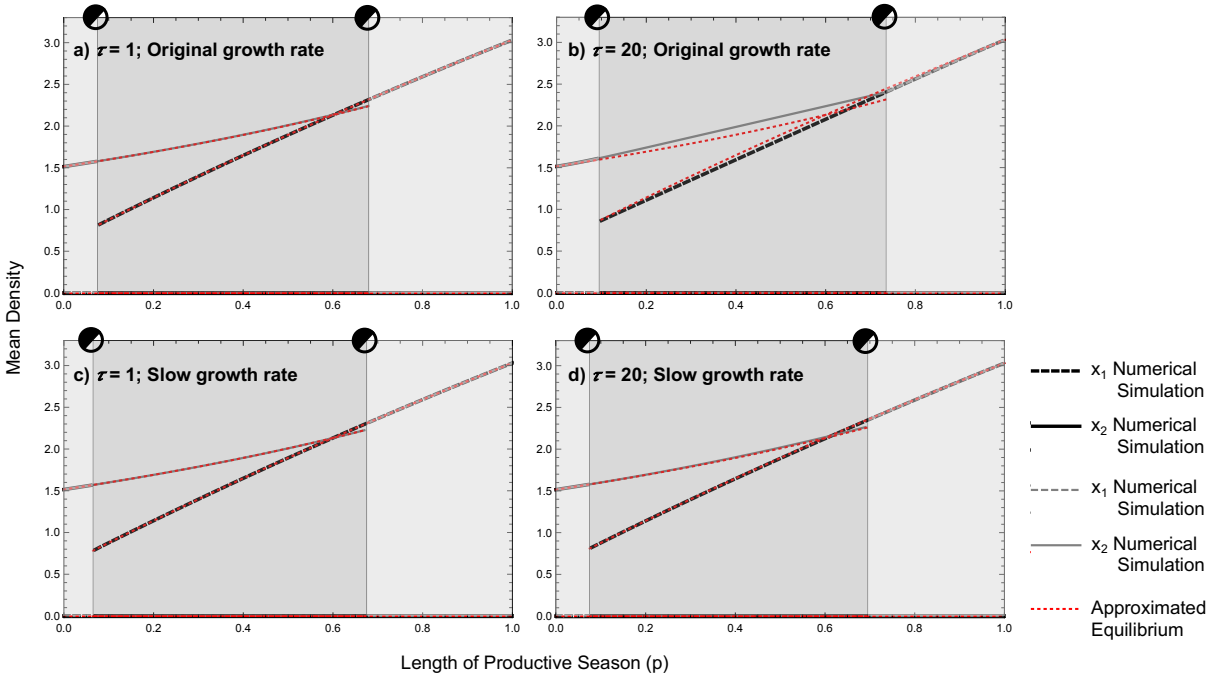

Fig. S4.31 Isocline approximation – mean density plots over the length of the productive season (p) for seasonally-mediated contingent coexistence. Light grey zones represent competitive exclusion and grey zones represent contingent coexistence. a) and b) original growth rates (those used throughout manuscript: $r_{P1} = 1.7$, $r_{P2} = 1.2$, $r_{LP1} = 1$, $r_{LP2} = 0.3$) when the period length $\tau =$ 1 and 20 time-units respectively. c) and d) all growth rates have been divided by 10 units ($r_{P1} =$ 0.17, $r_{P2} = 0.12$, $r_{LP1} = 0.1$, $r_{LP2} = 0.03$) when the period length = 1 and 20 time-units respectively. Parametric values: $\alpha_{P,21}$=0.548, $\alpha_{P,12}$=0.33, $\alpha_{P,11}$=0.33, $\alpha_{P,22}$=0.363, $\alpha_{LP,21}$=1.31, $\alpha_{LP,12}$=1.89, $\alpha_{LP,11}$=1.65, $\alpha_{LP,22}$=0.66.

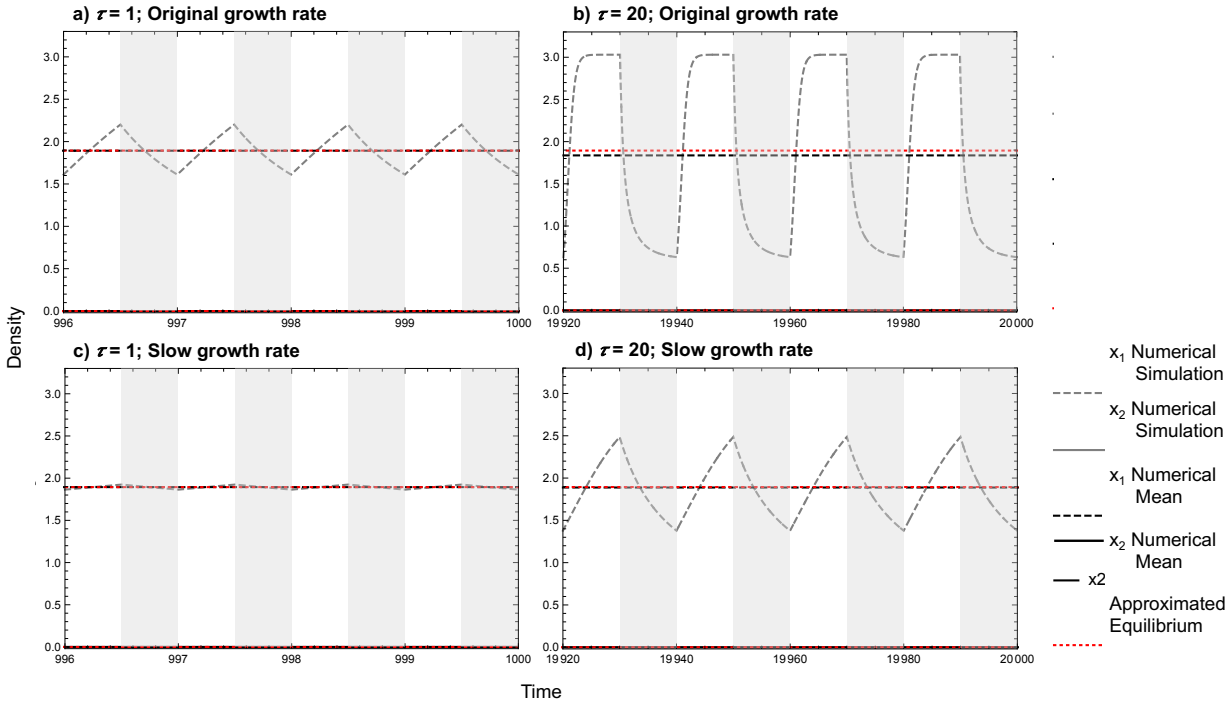

Fig. S4.32 Isocline approximation – time series for seasonally-mediated contingent coexistence. Length of productive season (p) = 0.5 represented by white zones, and light grey zones represent the less-productive season. a) and b) original growth rates (those used throughout manuscript: r_{P1} = 1.7, r_{P2} = 1.2, r_{LP1} = 1, r_{LP2} = 0.3) when the period length τ = 1 and 20 time-units respectively. c) and d) all growth rates have been divided by 10 units (r_{P1} = 0.17, r_{P2} = 0.12, r_{LP1} = 0.1, r_{LP2} = 0.03) when the period length = 1 and 20 time-units respectively. Parametric values: $\alpha_{P,21}$=0.548, $\alpha_{P,12}$=0.33, $\alpha_{P,11}$=0.33, $\alpha_{P,22}$=0.363, $\alpha_{LP,21}$=1.31, $\alpha_{LP,12}$=1.89, $\alpha_{LP,11}$=1.65, $\alpha_{LP,22}$=0.66.